

Fast and Powerful Conditional Randomization Testing via Distillation

Molei Liu¹ and Lucas Janson²

Abstract

In relating a response variable Y to covariates (Z, X) , a key question is whether Y is independent of the covariate X given Z . This question can be answered through *conditional independence testing*, and the conditional randomization test (CRT) was recently proposed by Candès et al. (2018) as a way to use distributional information about $X | Z$ to exactly (non-asymptotically) test for conditional independence between X and Y using *any* test statistic in *any* dimensionality without assuming anything about $Y | (Z, X)$. This flexibility in principle allows one to derive powerful test statistics from complex state-of-the-art machine learning algorithms while maintaining exact statistical control of Type 1 errors. Yet the direct use of such advanced test statistics in the CRT is prohibitively computationally expensive, especially with multiple testing, due to the CRT’s requirement to recompute the test statistic many times on resampled data. In this paper we propose a novel approach, called *distillation*, to using state-of-the-art machine learning algorithms in the CRT while drastically reducing the number of times those algorithms need to be run, thereby taking advantage of their power and the CRT’s statistical guarantees without suffering the usual computational expense associated with their use in the CRT. In addition to distillation, we propose a number of other tricks to speed up the CRT without sacrificing its strong statistical guarantees, and show in simulation that all our proposals combined lead to a test that has the same power as the CRT but requires orders of magnitude less computation, making it a practical and powerful tool even for large data sets. We demonstrate our method’s speed and power on a breast cancer dataset by identifying biomarkers related to cancer stage.

Keywords: Conditional Randomization Test (CRT), model-X, conditional independence testing, high-dimensional inference, machine learning.

1 Introduction

In our increasingly data-driven world, it has become the norm in applications from genetics and health care to policy evaluation and e-commerce to seek to understand the relationship between a response variable of interest and a high-dimensional set of potential explanatory variables or covariates. While accurately estimating this entire relationship generally would require a nearly-infinite sample size, a less-intractable but still extremely useful question is to ask, for any given covariate, whether it actually contributes to the response variable’s high-dimensional conditional distribution. We address this problem by encoding a covariate’s relevance in *conditional independence testing*, which requires no modeling assumptions to define. Denoting the response random variable by Y , a given covariate of interest by X , and a multidimensional set of further covariates by $Z = (Z_1, \dots, Z_p)$, then the null hypothesis we seek to test is

$$H_0 : Y \perp\!\!\!\perp X | Z$$

¹Department of Biostatistics, Harvard Chan School of Public Health.

²Department of Statistics, Harvard University.

against the alternative $H_1 : Y \not\perp X \mid Z$. Testing this hypothesis for just a single covariate is sometimes all that is needed, such as in an observational study investigating whether a particular treatment (X) causes a change in a response (Y) after controlling for a set of measured confounding variables (Z). But in other applications no one covariate holds *a priori* precedence over another, and a researcher is seeking any and all covariates that contribute to Y 's conditional distribution. This variable selection objective can also be achieved by testing H_0 for each covariate in turn and plugging the resulting p -values into one of the many well-established procedures from the deep literature on multiple testing. In addition to the considerable statistical challenge of providing a valid and powerful test of H_0 , it is of paramount importance to also ensure that test is computationally efficient, especially, as is often the case in modern applications, when either or both the sample size and dimension are large, and even more so when a variable selection objective requires the test to be run many times. Thus the goal of this paper is to present a test for conditional independence that is provably valid, empirically powerful, and computationally efficient.

1.1 Background

Our work builds on the *conditional randomization test* (CRT) introduced in Candès et al. (2018). The CRT is a very general framework for conditional independence testing that can leverage any test statistic one chooses and exactly (non-asymptotically) controls the Type I error regardless of the data dimensionality. The CRT's guarantees assume nothing whatsoever about $Y \mid (X, Z)$, but instead assume $X \mid Z$ is known. This so-called "model-X" framework (in contrast to the canonical approach of assuming a strong model for $Y \mid (X, Z)$) is perhaps easiest to justify when a wealth of *unlabeled data*¹ is available, but has also been found to be quite robust even when $X \mid Z$ is estimated by only the labeled data.

In order to define the CRT, we first need notation for our data. For $i \in \{1, \dots, n\}$, let $(Y_i, X_i, Z_i) \in \mathbb{R}^{p+2}$ be i.i.d. copies of (Y, X, Z) , and denote the column vector of Y_i 's by $\mathbf{y} \in \mathbb{R}^n$, the column vector of X_i 's by $\mathbf{x} \in \mathbb{R}^n$, and the matrix whose rows are the Z_i 's by $\mathbf{Z} \in \mathbb{R}^{n \times p}$. The CRT is given by Algorithm 1, and its Type I error guarantee follows below.

Algorithm 1 The conditional randomization test (CRT).

Input: Data $(\mathbf{y}, \mathbf{x}, \mathbf{Z})$, test statistic function T , and number of randomizations M .

for $m = 1, 2, \dots, M$ **do**

Sample $\mathbf{x}^{(m)}$ from the distribution of $\mathbf{x} \mid \mathbf{Z}$, conditionally independently of \mathbf{x} and \mathbf{y} .

end for

Output: CRT p -value $\frac{1}{M+1} \left(1 + \sum_{m=1}^M \mathbb{1}_{\{T(\mathbf{y}, \mathbf{x}^{(m)}, \mathbf{Z}) \geq T(\mathbf{y}, \mathbf{x}, \mathbf{Z})\}} \right)$.

Theorem 1 (Candès et al. (2018)). *Under H_0 , the CRT p -value q satisfies $\mathbb{P}(q \leq \alpha) \leq \alpha$ for all $\alpha \in [0, 1]$.*

For many common models of $X \mid Z$, the conditionally-independent sampling of $\mathbf{x}^{(m)}$ is straightforward. And even in more complex models it is still often easy to sample $\mathbf{x}^{(m)}$ conditionally-*exchangeably* with \mathbf{x} and conditionally-independently of \mathbf{y} (for instance by conditioning on an inferred latent variable), which is sufficient for Theorem 1 to hold. Because Theorem 1 only relies on the exchangeability of the vectors $\mathbf{x}, \mathbf{x}^{(1)}, \dots, \mathbf{x}^{(M)}$ under H_0 , it is entirely agnostic to the choice of test statistic T . This enables some very powerful choices, such as T 's derived from modern machine learning algorithms, from Bayesian inference (though neither the prior nor model for

¹Pairs (X_i, Z_i) without corresponding Y_i .

$Y \mid (X, Z)$ need be well-specified), or from highly-domain-specific knowledge or intuition. Unfortunately the most powerful statistics are often particularly expensive to compute, and as can be seen from Algorithm 1, T must be applied $M + 1$ times in order to compute a single p -value. When testing all the covariates at once, this computational problem is compounded as not only does *each* test require $M + 1$ applications of T , but M must be roughly of order p to ensure the p -values are sufficiently high-resolution to make any discoveries with standard multiple testing procedures such as Benjamini–Hochberg (Benjamini and Hochberg, 1995). For multiple testing, model-X knockoffs (Candès et al., 2018) provides an appealing alternative but can suffer relative to the CRT in terms of power, especially in very sparse settings; see Appendix A for details. This apparent conflict between computational tractability and statistical power presents a barrier to the widespread use of the CRT.

1.2 Our contribution

This paper resolves this conflict in Section 2 by introducing a technique we call *distillation* to the CRT that can still leverage *any* high-dimensional modeling or supervised learning algorithm, but presents dramatic computational savings by only requiring the expensive high-dimensional computation to be performed once, instead of $M + 1$ times. We call our proposed method the distilled CRT, or dCRT, and improve its computation further in Section 3 by describing two additional speedups that can be applied in certain common problem settings. One removes the need for resampling entirely and the other provides computational savings in multiple testing settings by focusing computation on only the most promising covariates. None of our proposed computational speedups change the exact, finite-sample Type I error control the dCRT inherits from the CRT. And we demonstrate in simulations in Section 4 that there is generally *no* power loss when comparing a dCRT to its more expensive CRT counterpart, while our proposals save orders of magnitude in computation even for medium-scale problems (the savings only increase for larger data). We also show in simulations that the dCRT is more powerful than other state-of-the-art conditional independence tests, and is also robust to misspecification in the distribution of X . Finally, in Section 5, we apply the dCRT to a breast cancer dataset and discover more clinically-informative somatic mutations than competing methods, and we cite independent scientific work corroborating each of the discoveries we make.

1.3 Related work

Our work builds upon the CRT of Candès et al. (2018), with the goal of making it computationally tractable without sacrificing power; see Janson (2017) for detailed discussion of the differences between this model-X line of work and the canonical approach that assumes a model for $Y \mid (X, Z)$. Our work is perhaps most similar to the HRT of Tansey et al. (2018), which uses data splitting to enable the use of complex modeling in the CRT with far less computation by doing all the complex modeling on the first part of the data and testing on the second part. A similar approach is adopted in Bates et al. (2020) who apply the CRT to genetic trio studies, and another sample-splitting extension of the HRT is introduced in Katsevich and Ramdas (2020) to enable power analysis. We show in Section 4 that data splitting comes with a substantial power loss compared to the original (slower) CRT and the dCRT. Tansey et al. (2018) addresses this with cross-fitting, but in doing so loses the guarantee on Type I error control of the CRT (and dCRT). Other works extending the CRT include Berrett et al. (2019); Bellot and van der Schaar (2019), but do not address its computational intractability. For multiple testing, model-X knockoffs (Candès et al., 2018) can simultaneously test conditional independence for each covariate. But as we show in Section 4, it

tends to be less powerful than the CRT, especially when there are few non-null covariates.

We note a pair of methods, double machine learning (DML) (Chernozhukov et al., 2016) and the generalized covariance measure (GCM) (Shah and Peters, 2018), that both test conditional independence under assumptions that nearly (but not quite, due to moment conditions on Y) subsume ours, and whose test statistic resembles and can even be identical to certain special cases of the dCRT. However, their statistics only resemble a special case of the dCRT—the dCRT framework includes many other statistics which deviate substantially from DML/GCM and can be more powerful in certain settings (see Appendices C.5 and C.7). Furthermore, the cutoffs for their test statistics are both based on asymptotic normality, while the dCRT is non-asymptotically exact regardless of the distribution of its test statistic (see Appendix C.4).

1.4 Notation

For any set of indices $J = (j_1, j_2, \dots, j_k) \subseteq \{1, 2, \dots, p\}$ and matrix $\mathbf{A} = (\mathbf{a}_1, \mathbf{a}_2, \dots, \mathbf{a}_p) \in \mathbb{R}^{n \times p}$ with $\mathbf{a}_j = (A_{1j}, A_{2j}, \dots, A_{nj})^\top$, we use \mathbf{A}_J and \mathbf{A}_{-J} to represent the matrices with columns given by those of \mathbf{A} whose indices belong to J and $\{1, 2, \dots, p\} \setminus J$, respectively. For a single index j , we define $\mathbf{A}_j := \mathbf{A}_{\{j\}}$ and $\mathbf{A}_{-j} := \mathbf{A}_{-\{j\}}$ for simplicity. For any two vectors \mathbf{a}_j and \mathbf{a}_ℓ , let $\mathbf{a}_j \odot \mathbf{a}_\ell = (A_{1j}A_{1\ell}, A_{2j}A_{2\ell}, \dots, A_{nj}A_{n\ell})^\top$ denote their element-wise product, and for $L = \{\ell_1, \ell_2, \dots, \ell_k\}$ let $\mathbf{a}_j \odot \mathbf{A}_L = (\mathbf{a}_j \odot \mathbf{a}_{\ell_1}, \dots, \mathbf{a}_j \odot \mathbf{a}_{\ell_k})$; these elementwise products will be used when fitting first-order interaction effects.

2 The distilled conditional randomization test

2.1 Main idea

It is natural to derive CRT test statistics from machine learning methods with high predictive and estimation accuracy. Indeed the original paper proposing the CRT (Candès et al., 2018) used the LASSO (Tibshirani, 1996) to derive a test statistic and found it to be quite powerful. Specifically, the test statistic was chosen to be $T_{\text{CRT}}(\mathbf{y}, \mathbf{x}, \mathbf{Z}) := |\hat{\beta}_x|$, the absolute value of the fitted coefficient on \mathbf{x} from the LASSO of \mathbf{y} on (\mathbf{x}, \mathbf{Z}) with penalty parameter chosen by cross-validation. Although powerful and computationally much faster than many other machine learning algorithms, it is still expensive to repeatedly run the LASSO on large data sets hundreds or more times just to compute a single p -value, and many times more than that in multiple-testing scenarios when a p -value for each covariate is needed.

Consider now the following alternative test statistic which captures the essence of our proposal. First fit a cross-validated LASSO of \mathbf{y} on \mathbf{Z} to obtain the p -dimensional coefficient vector $\hat{\beta}_{\mathbf{Z}}$. Then fit a least-squares regression of the residual $(\mathbf{y} - \mathbf{Z}\hat{\beta}_{\mathbf{Z}})$ on \mathbf{x} to obtain the scalar coefficient $\hat{\beta}'_x$ and take its absolute value $T_{\text{dCRT}}(\mathbf{y}, \mathbf{x}, \mathbf{Z}) := |\hat{\beta}'_x|$ as the test statistic. It may seem as though little has changed from the preceding paragraph—we would expect T_{CRT} and T_{dCRT} to have similar statistical properties and require nearly the same computation. Although the statistical properties of T_{CRT} and T_{dCRT} are indeed very similar and they do require nearly the same time to compute *once*, they require dramatically different computation within the CRT. The key difference is that the expensive $(p + 1)$ -dimensional LASSO fit in T_{CRT} must be recomputed for *each* resample of \mathbf{x} , while the expensive p -dimensional LASSO fit in T_{dCRT} must only be computed once, since that LASSO does not depend on \mathbf{x} and hence is identical for all its resamples. In the CRT, neither \mathbf{y} nor \mathbf{Z} change during the resampling procedure, and we take advantage of this by applying our expensive computation to only \mathbf{y} and \mathbf{Z} so it only has to be done once. All that is required for

each resample’s computation of T_{dCRT} is a *univariate* regression, whose computational expense is far lower than a p -dimensional LASSO.

We can generalize this idea far beyond the LASSO or linear regressions. The core proposal is to *distill* all the high-dimensional information in \mathbf{Z} about \mathbf{y} into a low-dimensional representation, without looking at \mathbf{x} . Then the test statistic estimates a relationship between \mathbf{x} and the *leftover* information in \mathbf{y} by only looking at \mathbf{x} , \mathbf{y} , and the distilled (low-dimensional) function of \mathbf{Z} . Thus all the computation on high-dimensional data, namely the distillation, only needs to be performed once, while the computation that is repeatedly applied to the resampled data is low-dimensional and hence relatively fast. It will often be advantageous to also distill the high-dimensional information in \mathbf{Z} about \mathbf{x} and include this in the test statistic as well, but we will see this can be done without looking at \mathbf{x} and hence does not require any repeated computation on the resampled $\mathbf{x}^{(m)}$.

2.2 Formal presentation of dCRT

We now formalize the idea from the previous subsection in Algorithm 2, the distilled conditional randomization test (dCRT).

Algorithm 2 The distilled conditional randomization test (dCRT).

Input: Data $(\mathbf{y}, \mathbf{x}, \mathbf{Z})$, \mathbf{y} -distillation-fitting function \mathcal{D}_y , \mathbf{x} -distillation function d_x , test statistic function T , and number of randomizations M .

Distill \mathbf{Z} ’s information about \mathbf{y} into $\mathbf{d}_y = \mathcal{D}_y(\mathbf{y}, \mathbf{Z})$ and about \mathbf{x} into $\mathbf{d}_x = d_x(\mathbf{Z})$.

for $m = 1, 2, \dots, M$ **do**

 Sample $\mathbf{x}^{(m)}$ from the distribution of $\mathbf{x} \mid \mathbf{Z}$, conditionally independently of \mathbf{x} and \mathbf{y} .

end for

Output: dCRT p -value $\frac{1}{M+1} \left(1 + \sum_{m=1}^M \mathbb{1}_{\{T(\mathbf{y}, \mathbf{x}^{(m)}, \mathbf{d}_y, \mathbf{d}_x) \geq T(\mathbf{y}, \mathbf{x}, \mathbf{d}_y, \mathbf{d}_x)\}} \right)$.

The key difference from the more general CRT in Algorithm 1 is that the test statistic function T in Algorithm 2 only sees information about the high-dimensional \mathbf{Z} through its \mathbf{y} - and \mathbf{x} -distillations \mathbf{d}_y and \mathbf{d}_x , which are both computed just once in the first line of the algorithm. \mathcal{D}_y and d_x should be chosen such that the distillation step produces \mathbf{d}_y and \mathbf{d}_x with dimension much less than p , so that T ’s inputs are low-dimensional. Then since T is the only repeatedly-applied function and its computation does not suffer from the high-dimensionality of the original data, the dCRT’s computation will be dominated by the single application of \mathcal{D}_y . For instance, in the dCRT example in Section 2.1, d_x is not used and \mathcal{D}_y fits a cross-validated LASSO of \mathbf{y} on \mathbf{Z} and returns $\mathbf{d}_y = \mathbf{Z}\hat{\beta}_z$, while $T(\mathbf{y}, \mathbf{x}, \mathbf{d}_y) = (\mathbf{y} - \mathbf{d}_y)^\top \mathbf{x} / \|\mathbf{x}\|^2$ requires negligible computation by comparison.

Note that \mathcal{D}_y and d_x , despite both producing distillations, operate quite differently. In particular, although d_x distills \mathbf{Z} ’s information about \mathbf{x} , it does not take \mathbf{x} as an argument. This is because the distillation function d_x can be chosen purely based on $X \mid Z$ which is assumed known, and thus can bypass looking at \mathbf{x} and distill \mathbf{Z} directly; for example, we will soon discuss dCRTs with $d_x(\mathbf{z}) = \mathbb{E}[\mathbf{x} \mid \mathbf{Z} = \mathbf{z}]$. In contrast, \mathcal{D}_y needs to internally *fit* a distillation function which we could think of as “ d_y ” (this is the expensive step) and then apply it to \mathbf{Z} to compute \mathbf{d}_y . This distinction between \mathcal{D}_y and d_x is important since if d_x performed a complicated fitting step that depended on \mathbf{x} , then that complicated computation would have to be repeated for each $\mathbf{x}^{(m)}$ in order to maintain the exchangeability of $\mathbf{x}, \mathbf{x}^{(1)}, \dots, \mathbf{x}^{(M)}$ under H_0 used in the proof of Theorem 1. Importantly, Theorem 1’s validity guarantee indeed applies to the dCRT because it is a special case of the CRT.

We emphasize that \mathcal{D}_y can really be *any* regression algorithm and Theorem 1 still holds. Thus it can take advantage of the predictive power of state-of-the-art machine learning algorithms, precise knowledge in the form of a Bayesian prior, or even imprecise domain expertise or intuition applied by trying many different regressions of \mathbf{y} on \mathbf{Z} and choosing whichever “feels” best (as long as \mathbf{x} is not factored into that decision). In the sequel we provide some suggestions and default choices.

2.3 Specific constructions

Algorithm 2 provides a framework for fast and powerful CRTs, but leaves much unspecified. In this section, we provide more detail on some ways that the dCRT can be implemented in different scenarios, and discuss their associated advantages and disadvantages.

2.3.1 The d₀CRT: fast, powerful, and intuitive

The most computationally-efficient and often the most intuitive class of dCRT procedures has both \mathbf{y} - and \mathbf{x} -distillations reduce \mathbf{Z} to an output with a single column. We label this subclass of dCRT procedures as d₀CRT because it represents the choice to maximally-distill each row of \mathbf{Z} down to a single scalar. Assuming T ’s computation generally increases with the dimension of its inputs, the d₀CRT also represents a particularly computationally-efficient class of dCRTs.

A natural approach to constructing a d₀CRT, especially when Y is continuous, is to have distillation take the form of conditional mean functions. That is, let $d_x(\mathbf{Z}) = \mathbb{E}[\mathbf{x} | \mathbf{Z}]$ and have \mathcal{D}_y fit an estimate of the analogous regression function for \mathbf{y} , i.e., $\mathcal{D}_y(\mathbf{y}, \mathbf{Z}) \approx \mathbb{E}[\mathbf{y} | \mathbf{Z}]$. Then T can be chosen as an empirical measure of dependence between the residuals $\mathbf{y} - \mathbf{d}_y$ and $\mathbf{x} - \mathbf{d}_x$, such as the square of the fitted coefficient when regressing the former on the latter. This approach is also easy to understand and implement since it just requires choosing \mathcal{D}_y and T , with \mathcal{D}_y just performing a (possibly nonparametric) regression while T can be thought of as computing a test statistic for testing the independence between two scalar random variables from a paired sample of size n : $(\mathbf{y} - \mathbf{d}_y, \mathbf{x} - \mathbf{d}_x)$. As both regression and bivariate independence testing are highly-studied topics, users can easily draw from their statistical training, domain expertise, and a rich literature in order to design an appropriate d₀CRT for their particular problem. As a generic example we found to be computationally efficient and powerful in our simulations, consider the following.

Example 1 (LASSO-based d₀CRT). *Let $\mathbf{d}_y = \mathbf{Z}\hat{\beta}_z$ be the fitted predictions from a cross-validated LASSO of \mathbf{y} on \mathbf{Z} , let $\mathbf{d}_x = \mathbb{E}[\mathbf{x} | \mathbf{Z}]$, and let $T(\mathbf{y}, \mathbf{x}, \mathbf{d}_y, \mathbf{d}_x) = \hat{\beta}_x^2 := \left(\frac{(\mathbf{y} - \mathbf{d}_y)^\top (\mathbf{x} - \mathbf{d}_x)}{\|\mathbf{x} - \mathbf{d}_x\|^2} \right)^2$.*

In spite of the intuitive appeal of couching distillation in terms of finding conditional means, in some problem instances an alternative d₀CRT may be more appropriate. For instance, an appealing analogue of Example 1 for binary Y might fit $\hat{\beta}_z$ by a cross-validated ℓ_1 -penalized logistic regression of \mathbf{y} on \mathbf{Z} and otherwise leave \mathcal{D}_y and \mathbf{d}_x unchanged (note $\mathbf{Z}\hat{\beta}_z$ no longer approximates $\mathbb{E}[\mathbf{y} | \mathbf{Z}]$), and take $T(\mathbf{y}, \mathbf{x}, \mathbf{d}_y, \mathbf{d}_x)$ to be the squared fitted coefficient from a logistic regression of \mathbf{y} on $\mathbf{x} - \mathbf{d}_x$ with offset \mathbf{d}_y . The substantial flexibility of the d₀CRT allows it to detect many kinds of nonlinear relationships between Y and X , but the stringent distillation inherently limits its ability to detect most types of *interactions* between X and Z . This shortcoming can be important and in the next subsection we discuss how interactions can be incorporated by moving beyond the d₀CRT.

2.3.2 The d₁CRT: discovering interactions

Of the three functions applied in Algorithm 2, only T takes both \mathbf{y} and \mathbf{x} as arguments and hence the choice of T is how a user can encode the kinds of non-null relationships between Y and X

that are deemed plausible or even likely. But because T only sees \mathbf{Z} through \mathbf{d}_y and \mathbf{d}_x , any plausible models for Y must be expressed using only \mathbf{x} , \mathbf{d}_y , and \mathbf{d}_x . This means in particular that the d_0 CRT has almost no capacity to model even first-order interactions between X and Z . For instance, suppose $p = 3$ and $Z_j \stackrel{i.i.d.}{\sim} \mathcal{N}(0, 1)$, $X \sim Z_1 + \mathcal{N}(0, 1)$, and $Y \sim Z_2 + XZ_3 + \mathcal{N}(0, 1)$. Then the best possible distillations of \mathbf{x} and \mathbf{y} are $\mathbf{d}_x = \mathbf{Z}_1$ and $\mathbf{d}_y = \mathbf{Z}_2 + \mathbf{Z}_1 \odot \mathbf{Z}_3$, respectively, making it impossible for T to encode the true conditional mean of \mathbf{y} , namely, $\mathbf{Z}_2 + \mathbf{x} \odot \mathbf{Z}_3$, from just \mathbf{x} , \mathbf{d}_x , and \mathbf{d}_y .

To address this limitation of the d_0 CRT, one can simply increase the dimension of \mathbf{d}_y and \mathbf{d}_x to explicitly include possible columns of \mathbf{Z} with which \mathbf{x} might be expected to interact. But of course increasing the dimension of \mathbf{d}_y and \mathbf{d}_x tends to come at a computational cost, since their low-dimensionality is exactly what makes the dCRT fast in the first place. Thus one needs some sort of prior, domain knowledge, or heuristic for choosing based on either the pair (\mathbf{y}, \mathbf{Z}) or (\mathbf{x}, \mathbf{Z}) (but not based on $(\mathbf{y}, \mathbf{x}, \mathbf{Z})$ together) a small subset of columns of \mathbf{Z} that \mathbf{x} might plausibly interact with. One option is to split the data into two independent parts and use one part in an unconstrained way to select columns of \mathbf{Z} that are likely to interact with \mathbf{x} , and then to leverage these selections in a dCRT run only on the other part. We propose here an alternative that avoids sample splitting, based on the common statistical practice of only allowing for interactions between variables with strong main effects. This practice of enforcing hierarchy in interactions has a long history in applied and theoretical statistics under many different names (Nelder, 1977; Cox, 1984; Peixoto, 1987; Hamada and Wu, 1992; Chipman, 1996; Bien et al., 2013).

Our proposed method for incorporating interactions, which we call the d_1 CRT, is to have \mathcal{D}_y still distill \mathbf{Z} into one column to best-capture the relationship between \mathbf{y} and \mathbf{Z} , but then to additionally return (as further columns of \mathbf{d}_y) a limited subset of columns of \mathbf{Z} whose contributions to that fitted relationship are strongest. Then T can be chosen as a test statistic that allows \mathbf{x} to interact with those columns of \mathbf{Z} contained in \mathbf{d}_y , while still prioritizing the main effect of \mathbf{x} . As a generic example we found to be powerful to detect hierarchical interactions without losing much power in the absence of interactions, consider the following.

Example 2 (LASSO-based d_1 CRT). *Let $\mathbf{d}_y = (\mathbf{Z}\hat{\beta}_z, \mathbf{Z}_{\text{top}(k)}) := (\mathbf{d}_{y,1}, \mathbf{d}_{y,-1})$ be the fitted predictions from a cross-validated LASSO of \mathbf{y} on \mathbf{Z} concatenated with the columns of \mathbf{Z} corresponding to the k largest entries of $|\hat{\beta}_z|$, let $\mathbf{d}_x = \mathbb{E}[\mathbf{x} | \mathbf{Z}]$, and let $T(\mathbf{y}, \mathbf{x}, \mathbf{d}_y, \mathbf{d}_x) = \hat{\beta}_{x,1}^2 + \frac{1}{k} \sum_{j=2}^{k+1} \hat{\beta}_{x,j}^2$, where $\hat{\beta}_x \in \mathbb{R}^{k+1}$ is the fitted coefficient vector from a least-squares fit of $(\mathbf{y} - \mathbf{d}_{y,1})$ on $(\mathbf{x} - \mathbf{d}_x)$ and $(\mathbf{x} - \mathbf{d}_x) \odot \mathbf{d}_{y,-1}$.*

The normalization by $1/k$ of $\sum_{j=2}^{k+1} \hat{\beta}_{x,j}^2$ encodes our hierarchical prioritization of the main effect $\hat{\beta}_{x,1}$ over the interaction effects. For small k we still expect the computation to be dominated by \mathcal{D}_y , but it also represents a statistical trade-off in how widely to search for interactions; we found the performance to be quite stable to k in our simulations, but set as a default $k = 2 \log(p)$. Note that k could also be chosen after looking at (\mathbf{y}, \mathbf{Z}) , and more generally, one can construct many different types of d_1 CRT. For instance, one can adapt Example 2 to binary Y in an analogous way as was done for Example 1 by replacing linear regressions with logistic regressions and using $\mathbf{d}_{y,1}$ as an offset in T . Or one could have \mathcal{D}_y and/or T use the predictions and default variable importance measures from a random forest. We explore some of these options in simulations in Section 4.

3 Additional speedups

3.1 A resampling-free dCRT

Distillation massively reduces the computation time of the CRT by only requiring a single evaluation of the by-far-most-expensive function \mathcal{D}_y . But it still requires $M + 1$ evaluations of T , which can sometimes still contribute nontrivially to the computation time, and requires the user to choose the tuning parameter M which trades off computation and statistical power. It turns out that in certain cases the simplicity of T in the dCRT can be leveraged to remove the resampling of $\mathbf{x}^{(m)}$ entirely and compute an exact p -value directly from the single function evaluation $T(\mathbf{y}, \mathbf{x}, \mathbf{d}_y, \mathbf{d}_x)$.

For intuition, suppose $X | Z \sim \mathcal{N}(Z^\top \beta, \sigma^2)$, and consider the d_0 CRT with T as in Example 1,

$$T(\mathbf{y}, \mathbf{x}, \mathbf{d}_y, \mathbf{d}_x) = \left(\frac{(\mathbf{y} - \mathbf{d}_y)^\top (\mathbf{x} - \mathbf{d}_x)}{\|\mathbf{x} - \mathbf{d}_x\|^2} \right)^2.$$

Then since the (d)CRT conditions on \mathbf{y} and \mathbf{Z} (and hence also \mathbf{d}_y and $\mathbf{d}_x = \mathbf{Z}\beta$),

$$(\mathbf{y} - \mathbf{d}_y)^\top (\mathbf{x} - \mathbf{d}_x) \sim \mathcal{N}\left(0, \sigma^2 \|\mathbf{y} - \mathbf{d}_y\|^2\right).$$

The denominator of T makes things a bit more complicated, but the nature of the statistic does not change much if we replace the denominator by its expectation or, equivalently (since multiplying T by a fixed constant has no effect on its resulting p -value), simply replace it by 1: $T'(\mathbf{y}, \mathbf{x}, \mathbf{d}_y, \mathbf{d}_x) = \left((\mathbf{y} - \mathbf{d}_y)^\top (\mathbf{x} - \mathbf{d}_x) \right)^2$. We then get immediately that the *exact* p -value (i.e., the p -value that would result from taking the limit as $M \rightarrow \infty$) can be computed as $2 \left(1 - \Phi \left(\frac{T'(\mathbf{y}, \mathbf{x}, \mathbf{d}_y, \mathbf{d}_x)}{\sigma \|\mathbf{y} - \mathbf{d}_y\|} \right) \right)$ without ever resampling $\mathbf{x}^{(m)}$, where Φ is the standard normal CDF.

The same principle can be applied to non-Gaussian X : since the distribution of $(\mathbf{x} - \mathbf{d}_x) | \mathbf{Z}$ is known and the rows are independent, $(\mathbf{x} - \mathbf{d}_x)$ can be element-wise transformed via scalar monotone functions to be i.i.d. $\mathcal{N}(0, 1)$ given \mathbf{Z} . For conditionally-continuously-distributed $(\mathbf{x} - \mathbf{d}_x)$, this can be done via the probability inverse transform, while for distributions with atoms the atoms need to be carefully randomized (though just once); see Appendix B for details.

As long as $(\mathbf{x} - \mathbf{d}_x)$ is independent Gaussian or transformed to be, the same principle can also be applied to some more complex T functions. For instance, in Example 2, we can again replace the random “denominator” (in this case the matrix inverse in the least-squares formula for $\hat{\beta}_x$) with its conditional expectation given \mathbf{Z} , and end up with a quadratic form in Gaussian random variables. Efficient algorithms for computing the quantiles of a quadratic form in Gaussian random variables exist (Duchesne and De Micheaux, 2010) and can be applied to again compute the exact dCRT p -value without any resampling; see Appendix B for details.

3.2 Computational dimensionality reduction (CDR)

Conditional independence testing is often done in the context of a variable selection problem, wherein a p -value is needed for each covariate. Letting p now refer to the *total* number of covariates, this can be achieved by, for each column of the design matrix, treating that column as $\mathbf{x} \in \mathbb{R}^n$ and the remaining columns as $\mathbf{Z} \in \mathbb{R}^{n \times p-1}$ and applying the (d)CRT to compute a p -value. But then \mathcal{D}_y would need to be computed p times in total, once for each dCRT, creating a prohibitively-high computational burden in fields like genomics with high-dimensional covariates, even with all the speedups presented so far. A natural solution to this computational problem is to first use the

data to identify a preliminary subset of promising covariates, and then compute (d)CRT p -values for only that subset while setting the p -values for all the other covariates to 1. For instance, one could fit a cross-validated LASSO of \mathbf{y} on all the covariates and label only those with nonzero fitted coefficients as “promising”.

Unfortunately, in general, a screening step like this applied before the (d)CRT breaks the exchangeability between the original and resampled test statistics which Theorem 1 relies on to guarantee p -value validity. The intuitive reason for the failure of exchangeability is that the screening, when it discards covariates, takes a (data-dependent, and thus random) subset of covariates and implicitly changes their (d)CRT test statistics to ensure a p -value of 1 is returned. Hence, the screening implies an \mathbf{x} -dependent choice of T , whose distribution under the null will then be different when its argument is \mathbf{x} versus $\mathbf{x}^{(m)}$. But it turns out that despite this failure of exchangeability, the screening can only inflate a p -value and thus does not affect its validity, as we prove next by a simple argument.

Theorem 2. *Let $S(\mathbf{y}, \mathbf{x}, \mathbf{Z})$ be a screening function that equals 1 if \mathbf{x} is screened out and 0 otherwise, and let $q(\mathbf{y}, \mathbf{x}, \mathbf{Z})$ be a p -value produced by any (d)CRT. Then under H_0 , the screened p -value is given by $q'(\mathbf{y}, \mathbf{x}, \mathbf{Z}) = \max\{q(\mathbf{y}, \mathbf{x}, \mathbf{Z}), S(\mathbf{y}, \mathbf{x}, \mathbf{Z})\}$ and satisfies, for any $u \in [0, 1]$,*

$$\mathbb{P}(q'(\mathbf{y}, \mathbf{x}, \mathbf{Z}) \leq u) \leq u.$$

Proof.

$$\mathbb{P}(\max\{q(\mathbf{y}, \mathbf{x}, \mathbf{Z}), S(\mathbf{y}, \mathbf{x}, \mathbf{Z})\} \leq u) \leq \mathbb{P}(q(\mathbf{y}, \mathbf{x}, \mathbf{Z}) \leq u) \leq u.$$

□

Thus with the small computational overhead of a single well-chosen screening function (the screening will generally be a single computation such as a LASSO fit that returns the value of $S(\mathbf{y}, \mathbf{x}, \mathbf{Z})$ for *all* the covariates simultaneously), we can expect to dramatically cut the computation time of using the (d)CRT for variable selection. Note that the screening procedure increases the p -values relative to its unscreened analogue, but it nevertheless has no impact on power as long as it does not screen away any non-null p -values *that would have been rejected*, which is far less-stringent and more achievable than requiring the screening not to screen away *any* non-null p -values, and indeed we found in our simulations that simple screenings were able to substantially decrease computation time without affecting the power.

4 Simulations

In the interest of space we defer the details of our myriad simulations to the appendix and present here a detailed summary of the takeaways of those simulations, directly linking each takeaway to the figure and section of the appendix with the corresponding simulation(s) supporting it. The main focus of our simulations is examining the performance of the dCRT through the d₀CRT and d₁CRT given by Examples 1 and 2, respectively. Except where explicitly stated otherwise, we apply them in a resampling-free manner per Section 3.1 and, when simulating a variable selection task, with computational dimensionality reduction (using the cross-validated LASSO for selection) per Section 3.2. For variable selection simulations, we apply the BH procedure to each of the p -value methods (CRT, dCRT, HRT, DML, CGM). The BH procedure is only guaranteed to control the FDR under certain p -value-dependence assumptions which are not generally satisfied here, but it has been found to be quite robust in practice and indeed we find no evidence of FDR violations due to misapplication of BH; see Appendix C.11 for details. Source code for running dCRT can be found along with an example scripts for illustration at <https://github.com/moleibobliu/Distillation-CRT>.

Distillation dramatically reduces CRT computation without affecting power. In simulations with linear and logistic regression models, a range of signal amplitudes, and $n = p = 300$ (the data size was deliberately limited to accommodate the computational burden of the original CRT), both the d_0 CRT and d_1 CRT conferred a computational savings of approximately 500 times over the original CRT (Table A1) while having power nearly indistinguishable from (if anything slightly higher than) it (Figure A1). See Appendix C.2 for details.

The dCRT is more powerful than other fast model-X methods. In both the aforementioned $n = p = 300$ simulations and a larger simulation with $n = p = 800$, the dCRT computation times were mostly within an order of magnitude of the HRT and knockoffs (Tables A1 and A2). But across settings that included a range of n up to 1400, a range of p up to 3200, a range of signal magnitudes, a range of sparsities, a range of covariance structures for X , and a range of models for $Y | X$, both dCRT methods had consistently and substantially higher power than both the HRT (up to about 70 percentage points higher) and knockoffs (up to about 30 percentage points higher in less-sparse settings; in very sparse settings knockoffs becomes powerless and the dCRT can have arbitrarily-higher power than it) (Figures A1, A2, and A3). See Appendices C.2 and C.3 for details.

Double machine learning and the generalized covariance measure perform nearly identically to the d_0 CRT except when $Y | X, Z$ has heavy tails, in which case DML and GCM fail to control the Type I error. We applied DML and GCM in nearly all the simulations we ran, and found their performances so similar to the d_0 CRT that we did not bother plotting them. Their computation times were also similar to the dCRT (with DML’s somewhat higher due to cross-fitting). Recall however that both DML and GCM rely on asymptotic normality and hence require both large samples and well-behaved tails (unlike the dCRT which is exact for any n and any data distribution); indeed when we simulated $Y | X, Z$ to have a Laplace distribution and set $n = 30$, DML’s and GCM’s Type I error was inflated to about 150% of nominal (Figure A4). And, of course, in settings in which the d_1 CRT has higher power than the d_0 CRT, it similarly outperforms DML and GCM (Figures A7, A5). See Appendices C.4, C.5 and C.7 for details.

The d_1 CRT is stable to the choice of k and has slightly less power than the d_0 CRT in additive models but can have substantially higher power in the presence of interactions. In a simulation with an additive model, the power of the d_1 CRT was identical as k ranged from 2–22 (the default value of $k = 2 \log(p)$ would have been 13), while in a model with five true interactions, the power only varied from about 50% to about 40% over the same range of k (Figure A6). Throughout all our simulations in additive models we found the d_0 CRT to be slightly but consistently more powerful than the d_1 CRT (e.g., Figures A1, A2, A3, A8, A9), but in the presence of interactions obeying the hierarchy principle discussed in Section 2.3.2, we found that the d_1 CRT could be quite a bit more powerful (up to about 25 percentage points) than the d_0 CRT (Figure A5). See Appendices C.5 and C.6 for details.

The dCRT can leverage nonparametric machine learning algorithms for substantial power gains in highly-nonlinear models. In a simulation in which X ’s relationship with Y was highly-nonlinear and interacted with five Z_j ’s, our default (LASSO-based) d_1 CRT had somewhat higher power than d_0 CRT (as much as about 20 percentage points), but a different, random-forest-based d_1 CRT had far higher power than the LASSO-based d_1 CRT (as much as about 50 percentage points) (Figure A7). See Appendix C.7 for details.

The dCRT is quite robust to misspecification of X 's distribution. When the distribution of $X | Z$ is Poisson even with a very small mean parameter (making it highly discrete and heavily skewed) but approximated by a Gaussian with matching mean and variance, both the d_0 CRT and d_1 CRT maintain Type I error control and high power (Figure A8). Furthermore, when the covariates are jointly Gaussian but their covariance matrix is estimated in-sample, the Type I error of both dCRT methods does not inflate much above the nominal level even when a quite poor estimator is used (Figure A9). See Appendix C.8 for details.

The resampling-free versions of the dCRT are faster and just as powerful as the non-resampling-free dCRT except when $X | Z$ is highly discrete. The conversion to resampling-free sped up the d_0 CRT by 2.5 times in an $n = p = 800$ simulation and sped up the d_1 CRT by 11 times in an $n = p = 800$ simulation, even after applying CDR (Table A3). When $X | Z$ is Gaussian, changing the form of the test statistics of the d_0 CRT and d_1 CRT as proposed in paragraphs 2 and 4, respectively, of Section 3.1 had a negligible effect on their power (Figure A10). When $X | Z$ is non-Gaussian and must be transformed to Gaussian as described in paragraph 3 of Section 3.1, we found essentially no power loss for the resampling-free d_0 CRT and d_1 CRT relative to their non-resampling-free counterparts when $X | Z$ was Gamma-distributed (with shape = 3 and rate = 0.5, so that skew > 1 and excess kurtosis = 2), while there was substantial power loss (up to about 40 percentage points) when $X | Z$ was binary and hence required substantial exogenous randomization to be transformed to Gaussian, though the resampling-free dCRTs were still substantially more powerful (up to about 40 percentage points) than the HRT (Figure A11). See Appendix C.9 for details.

Computational dimensionality reduction makes the dCRT faster without affecting its power. In a simulation with $n = p = 800$, CDR reduced the computation time by a factor of about 5 for both d_0 CRT and d_1 CRT (Table A4) without perceptively changing their power (Figure A12). See Appendix C.10 for details.

5 Identifying biomarkers for breast cancer

As a final demonstration of the effectiveness of the dCRT, we apply it to a data set consisting of $n = 1,396$ staged oestrogen-receptor-positive cases of breast cancer, each with expression level (mRNA) and copy number aberration (CNA) measured for $p = 173$ genes (Pereira et al., 2016). Our goal is to find genes on which cancer stage depends, conditional on the remaining genes and all CNAs, while controlling the FDR at level 0.1. The discovery of such biomarkers for cancer can reveal new pathways and mechanisms for cancer progression; see Shen et al. (2019) for a recent application of model-X knockoffs to achieve the same goal.

After log-transforming the gene expressions, we modeled them as multivariate Gaussian conditional on their CNAs as in Solvang et al. (2011); Lahti et al. (2012); Leday et al. (2013). We applied the d_0 CRT, the d_1 CRT, the original LASSO-based CRT, the HRT, and model-X knockoffs and compared the results. See Appendix D for details of the data pre-processing, covariate-modeling, and method implementations. Table 1 contains the numbers of discoveries and runtimes (in R) for all the methods, showing that the dCRTs are the only model-X methods that are both fast and powerful on this data set. In particular, the original CRT takes over 5 hours to run while the dCRTs take under a minute, the HRT and knockoffs make one and zero discoveries, respectively. Knockoffs' lack of power can be attributed to the sparsity of discoverable genes, as mentioned in Section 1.1 and detailed in Appendix A.

Method	Discoveries	Time (minutes)
d ₀ CRT	5	0.5
d ₁ CRT	5	0.5
CRT	4	333.4
HRT	1	1.1
Knockoffs	0	0.1

Table 1: Numbers of discoveries and computation times (in R) of different methods in the breast cancer application.

It turns out that all five genes discovered by the dCRT (*FBXW7*, *MAP3K1*, *HRAS*, *GPS2*, and *RUNX1*; see Appendix A5 for their corresponding p -values) have been linked in independent research to cancer, suggesting the dCRT is making at least promising discoveries. In particular, *FBXW7* encodes a member of the F-box protein family and its mutations are detected in ovarian and breast cancer cell lines (Liu et al., 2019; Kirzinger et al., 2019); *MAP3K1* encodes a serine/threonine kinase on the NF-kappa-B and ERK and JNK kinase pathways, acting as a regulator for breast cancer (Glubb et al., 2015); *HRAS* belongs to the RAS oncogene family which is related to the transforming of genes of mammalian sarcoma retroviruses, and defects in this gene have been implicated in a variety of cancers (Geyer et al., 2018); over-expression of *GPS2* in mammalian cells may suppress signals mediated by RAS/MAPK and interfere with JNK activity, all of which are cancer-related (Jarmalavicius et al., 2010; Huang et al., 2016); *RUNX1* has been found to activate certain signaling pathways that promote tumor metastasis (Li et al., 2019).

6 Acknowledgements

We would like to thank Siyuan Ma, Wenshuo Wang, Dae Woong Ham, and Lu Zhang for helpful discussions and feedback on the paper.

References

- Barber, R. F. and Candès, E. J. (2015). Controlling the false discovery rate via knockoffs. *The Annals of Statistics*, 43(5):2055–2085.
- Bates, S., Sesia, M., Sabatti, C., and Candès, E. (2020). Causal inference in genetic trio studies. *arXiv preprint arXiv:2002.09644*.
- Bellot, A. and van der Schaar, M. (2019). Conditional independence testing using generative adversarial networks. In *Advances in Neural Information Processing Systems*, pages 2199–2208.
- Benjamini, Y. and Hochberg, Y. (1995). Controlling the false discovery rate: a practical and powerful approach to multiple testing. *Journal of the Royal statistical society: series B (Methodological)*, 57(1):289–300.
- Berrett, T. B., Wang, Y., Barber, R. F., and Samworth, R. J. (2019). The conditional permutation test for independence while controlling for confounders. *Journal of the Royal Statistical Society: Series B (Statistical Methodology)*.
- Bien, J., Taylor, J., and Tibshirani, R. (2013). A lasso for hierarchical interactions. *Annals of statistics*, 41(3):1111.

- Candès, E., Fan, Y., Janson, L., and Lv, J. (2018). Panning for gold: model-X knockoffs for high dimensional controlled variable selection. *Journal of the Royal Statistical Society: Series B (Statistical Methodology)*, 80(3):551–577.
- Chernozhukov, V., Chetverikov, D., Demirer, M., Duflo, E., Hansen, C., and Newey, W. K. (2016). Double machine learning for treatment and causal parameters. Technical report, Cemmap working paper.
- Chipman, H. (1996). Bayesian variable selection with related predictors. *Canadian Journal of Statistics*, 24(1):17–36.
- Cox, D. R. (1984). Interaction. *International Statistical Review/Revue Internationale de Statistique*, pages 1–24.
- Davies, R. B. (1980). Algorithm as 155: The distribution of a linear combination of χ^2 random variables. *Journal of the Royal Statistical Society. Series C (Applied Statistics)*, 29(3):323–333.
- Duchesne, P. and De Micheaux, P. L. (2010). Computing the distribution of quadratic forms: Further comparisons between the Liu–Tang–Zhang approximation and exact methods. *Computational Statistics & Data Analysis*, 54(4):858–862.
- Friedman, J., Hastie, T., and Tibshirani, R. (2008). Sparse inverse covariance estimation with the graphical lasso. *Biostatistics*, 9(3):432–441.
- Geyer, F. C., Li, A., Papanastasiou, A. D., Smith, A., Selenica, P., Burke, K. A., Edelweiss, M., Wen, H. C., Piscuoglio, S., and Schultheis, A. M. (2018). Recurrent hotspot mutations in HRAS-Q61 and PI3K-AKT pathway genes as drivers of breast adenomyoepitheliomas. *Nature communications*, 9(1):1–16.
- Glubb, D. M., Maranian, M. J., Michailidou, K., Pooley, K. A., Meyer, K. B., Kar, S., Carlebur, S., O’Reilly, M., Betts, J. A., Hillman, K. M., Kaufmann, S., Beesley, J., Canisius, S., Hopper, J. L., Southey, M. C., Tsimiklis, H., Apicella, C., Schmidt, M. K., Broeks, A., Hogervorst, F. B., van der Schoot, C. E., Muir, K., Lophatananon, A., Stewart-Brown, S., Siriwanarangsana, P., Fasching, P. A., Ruebner, M., Ekici, A. B., Beckmann, M. W., Peto, J., dos Santos-Silva, I., Fletcher, O., Johnson, N., Pharoah, P. D. P., Bolla, M. K., Wang, Q., Dennis, J., Sawyer, E. J., Tomlinson, I., Kerin, M. J., Miller, N., Burwinkel, B., Marme, F., Yang, R., Surowy, H., Gunel, P., Truong, T., Menegaux, F., Sanchez, M., Bojesen, S. E., Nordestgaard, B. G., Nielsen, S. F., Flyger, H., Gonzalez-Neira, A., Benitez, J., Zamora, M. P., Arias Perez, J. I., Anton-Culver, H., Neuhausen, S. L., Brenner, H., Dieffenbach, A. K., Arndt, V., Stegmaier, C., Meindl, A., Schmutzler, R. K., Brauch, H., Ko, Y.-D., Brning, T., Network, G., Nevanlinna, H., Muranen, T. A., Aittomaki, K., Blomqvist, C., Matsuo, K., Ito, H., Iwata, H., Tanaka, H., Drk, T., Bogdanova, N. V., Helbig, S., Lindblom, A., Margolin, S., Mannermaa, A., Kataja, V., Kosma, V.-M., Hartikainen, J. M., kConFab Investigators, Wu, A. H., Tseng, C.-c., Van Den Berg, D., Stram, D. O., Lambrechts, D., Zhao, H., Weltens, C., van Limbergen, E., Chang-Claude, J., Flesch-Janys, D., Rudolph, A., Seibold, P., Radice, P., Peterlongo, P., Barile, M., Capra, F., Couch, F. J., Olson, J. E., Hallberg, E., Vachon, C., Giles, G. G., Milne, R. L., McLean, C., Haiman, C. A., Henderson, B. E., Schumacher, F., Le Marchand, L., Simard, J., Goldberg, M. S., Labrche, F., Dumont, M., Teo, S. H., Yip, C. H., See, M.-H., Cornes, B., Cheng, C.-Y., Ikram, M. K., Kristensen, V., Study, N. B. C., Zheng, W., Halverson, S. L., Shrubsole, M., Long, J., Winqvist, R., Pylks, K., Jukkola-Vuorinen, A., Kauppila, S., Andrulis, I. L., Knight, J. A., Glendon, G., Tchatchou, S., Devilee, P., Tollenaar, R. A. E. M., Seynaeve, C., Van Asperen, C. J., Garca-Closas, M.,

- Figuerola, J., Chanock, S. J., Lissowska, J., Czene, K., Klevebring, D., Darabi, H., Eriksson, M., Hooning, M. J., Hollestelle, A., Martens, J. W. M., Colle, J. M., Hall, P., Li, J., Humphreys, K., Shu, X.-O., Lu, W., Gao, Y.-T., Cai, H., Cox, A., Cross, S. S., Reed, M. W. R., Blot, W., Signorello, L. B., Cai, Q., Shah, M., Ghoussaini, M., Kang, D., Choi, J.-Y., Park, S. K., Noh, D.-Y., Hartman, M., Miao, H., Lim, W. Y., Tang, A., Hamann, U., Torres, D., Jakubowska, A., Lubinski, J., Jaworska, K., Durda, K., Sangrajrang, S., Gaborieau, V., Brennan, P., McKay, J., Olsword, C., Slager, S., Toland, A. E., Yannoukakos, D., Shen, C.-Y., Wu, P.-E., Yu, J.-C., Hou, M.-F., Swerdlow, A., Ashworth, A., Orr, N., Jones, M., Pita, G., Alonso, M. R., Ivaréz, N., Herrero, D., Tessier, D. C., Vincent, D., Bacot, F., Luccarini, C., Baynes, C., Ahmed, S., Healey, C. S., Brown, M. A., Ponder, B. A. J., Chenevix-Trench, G., Thompson, D. J., Edwards, S. L., Easton, D. F., Dunning, A. M., and French, J. D. (2015). Fine-scale mapping of the 5q11.2 breast cancer locus reveals at least three independent risk variants regulating MAP3K1. *The American Journal of Human Genetics*, 96(1):5–20.
- Hamada, M. and Wu, C. J. (1992). Analysis of designed experiments with complex aliasing. *Journal of Quality Technology*, 24(3):130–137.
- Huang, J., Ma, S., and Zhang, C.-H. (2008). Adaptive lasso for sparse high-dimensional regression models. *Statistica Sinica*, pages 1603–1618.
- Huang, X., Xiao, F., Wang, S., Yin, R., Lu, C., Li, Q., Liu, N., Wang, L., and Li, P. (2016). G protein pathway suppressor 2 (GPS2) acts as a tumor suppressor in liposarcoma. *Tumor Biology*, 37(10):13333–13343.
- Imhof, J. P. (1961). Computing the distribution of quadratic forms in normal variables. *Biometrika*, 48(3/4):419–426.
- Janson, L. (2017). *A Model-Free Approach to High-Dimensional Inference*. PhD thesis, Stanford University.
- Jarmalavicius, S., Trefzer, U., and Walden, P. (2010). Differential arginine methylation of the G-protein pathway suppressor GPS-2 recognized by tumor-specific T-cells in melanoma. *The FASEB Journal*, 24(3):937–946.
- Katsevich, E. and Ramdas, A. (2020). A theoretical treatment of conditional independence testing under model-X. *arXiv preprint arXiv:2005.05506*.
- Kirzinger, M. W., Vizeacoumar, F. S., Haave, B., Gonzalez Lopez, C., Bonham, K., Kusalik, A., and Vizeacoumar, F. J. (2019). Humanized yeast genetic interaction mapping predicts synthetic lethal interactions of FBXW7 in breast cancer. *BMC medical genomics*, 12(1):112.
- Lahti, L., Schäfer, M., Klein, H. U., Bicciato, S., and Dugas, M. (2012). Cancer gene prioritization by integrative analysis of mRNA expression and dna copy number data: a comparative review. *Briefings in bioinformatics*, 14(1):27–35.
- Leday, G. G., van der Vaart, A. W., van Wieringen, W. N., and van de Wiel, M. A. (2013). Modeling association between DNA copy number and gene expression with constrained piecewise linear regression splines. *The Annals of Applied Statistics*, pages 823–845.
- Li, Q., Lai, Q., He, C., Fang, Y., Yan, Q., Zhang, Y., Wang, X., Gu, C., Wang, Y., Ye, L., Han, L., Lin, X., Chen, J., Cai, J., Li, A., and Liu, S. (2019). RUNX1 promotes tumour metastasis by activating the Wnt/ β -catenin signalling pathway and EMT in colorectal cancer. *Journal of Experimental & Clinical Cancer Research*, 38(1):334.

- Liu, F., Zou, Y., Wang, F., Yang, B., Zhang, Z., Luo, Y., Liang, M., Zhou, J., and Huang, O. (2019). FBXW7 mutations promote cell proliferation, migration, and invasion in cervical cancer. *Genetic testing and molecular biomarkers*, 23(6):409–417.
- Liu, H., Tang, Y., and Zhang, H. H. (2009). A new chi-square approximation to the distribution of non-negative definite quadratic forms in non-central normal variables. *Computational Statistics & Data Analysis*, 53(4):853–856.
- Nelder, J. (1977). A reformulation of linear models. *Journal of the Royal Statistical Society: Series A (General)*, 140(1):48–63.
- Peixoto, J. L. (1987). Hierarchical variable selection in polynomial regression models. *The American Statistician*, 41(4):311–313.
- Pereira, B., Chin, S.-F., Rueda, O. M., Vollan, H.-K. M., Provenzano, E., Bardwell, H. A., Pugh, M., Jones, L., Russell, R., Sammut, S.-J., Tsui, D. W. Y., Liu, B., Dawson, S.-J., Abraham, J., Northen, H., Peden, J. F., Mukherjee, A., Turashvili, G., Green, A. R., McKinney, S., Oloumi, A., Shah, S., Rosenfeld, N., Murphy, L., Bentley, D. R., Ellis, I. O., Purushotham, A., Pinder, S. E., Brresen-Dale, A.-L., Earl, H. M., Pharoah, P. D., Ross, M. T., Aparicio, S., and Caldas, C. (2016). The somatic mutation profiles of 2,433 breast cancers refine their genomic and transcriptomic landscapes. *Nature communications*, 7:11479.
- Shah, R. D. and Peters, J. (2018). The hardness of conditional independence testing and the generalised covariance measure. *Annals of Statistics*, to appear.
- Shen, A., Fu, H., He, K., and Jiang, H. (2019). False discovery rate control in cancer biomarker selection using knockoffs. *Cancers*, 11(6):744.
- Solvang, H. K., Lingjærde, O. C., Frigessi, A., Børresen Dale, A. L., and Kristensen, V. N. (2011). Linear and non-linear dependencies between copy number aberrations and mRNA expression reveal distinct molecular pathways in breast cancer. *BMC bioinformatics*, 12(1):197.
- Tansey, W., Veitch, V., Zhang, H., Rabadan, R., and Blei, D. M. (2018). The holdout randomization test: Principled and easy black box feature selection. *arXiv preprint arXiv:1811.00645*.
- Tibshirani, R. (1996). Regression shrinkage and selection via the lasso. *Journal of the Royal Statistical Society: Series B (Methodological)*, 58(1):267–288.
- Zou, H. (2006). The adaptive lasso and its oracle properties. *Journal of the American statistical association*, 101(476):1418–1429.
- Zou, H. and Hastie, T. (2005). Regularization and variable selection via the elastic net. *Journal of the royal statistical society: series B (statistical methodology)*, 67(2):301–320.

A The power of model-X knockoffs under strong sparsity

Model-X knockoffs uses the Selective SeqStep+ procedure with threshold $c = 0.5$ (Barber and Candès, 2015) in its final step, which cannot make a positive number of rejections fewer than $1/q$, where q is the nominal FDR level. Thus, if model-X knockoffs cannot make at least 10 discoveries while controlling the FDR at level $q = 0.1$, then it must make zero discoveries. So, for instance, if there are only 5 non-null covariates, model-X knockoffs will be nearly powerless to discover them, no matter how strong their relationships with Y .

B Resampling-free dCRT

B.1 Resampling-free LASSO-based d₁CRT

In this section, we describe the resampling-free version of the LASSO-based d₁CRT of Example 2 for gaussian X , in analog to the resampling-free d₀CRT detailed in Section 3.1. We follow the notation of Example 2 and for any $\mathbf{a} = (a_1, \dots, a_n)^\top \in \mathbb{R}^n$, let $\text{diag}(\mathbf{a})$ denote the diagonal matrix with its (i, i) -th entry being a_i for $i = 1, 2, \dots, n$. Then in Example 2,

$$\begin{aligned} \hat{\beta}_x &= \left[(\mathbf{1}, \mathbf{Z}_{\text{top}(k)})^\top \text{diag}^2(\boldsymbol{\epsilon}_x) (\mathbf{1}, \mathbf{Z}_{\text{top}(k)}) \right]^{-1} (\mathbf{1}, \mathbf{Z}_{\text{top}(k)})^\top \text{diag}(\boldsymbol{\epsilon}_x) (\mathbf{y} - \mathbf{d}_y) \\ &= \hat{\mathbb{H}}^{-1} (\mathbf{1}, \mathbf{Z}_{\text{top}(k)})^\top \text{diag}(\mathbf{y} - \mathbf{d}_y) \boldsymbol{\epsilon}_x, \end{aligned}$$

where $\hat{\mathbb{H}} = (\mathbf{1}, \mathbf{Z}_{\text{top}(k)})^\top \text{diag}^2(\boldsymbol{\epsilon}_x) (\mathbf{1}, \mathbf{Z}_{\text{top}(k)})$ and $\boldsymbol{\epsilon}_x = \mathbf{x} - \mathbf{d}_x$. And the test statistics

$$T(\mathbf{y}, \mathbf{x}, \mathbf{d}_y, \mathbf{d}_x) = \hat{\beta}_{x,1}^2 + \frac{1}{k} \sum_{j=2}^{k+1} \hat{\beta}_{x,j}^2 = \|\hat{\mathbb{H}}^{-1} \tilde{\mathbf{Z}}_{\text{top}(k)} \boldsymbol{\epsilon}_x\|_2^2$$

where $\tilde{\mathbf{Z}}_{\text{top}(k)} = (\mathbf{1}, k^{-1/2} \mathbf{Z}_{\text{top}(k)})^\top \text{diag}(\mathbf{y} - \mathbf{d}_y)$. In analog to the resampling-free d₀CRT introduced in Section 3.1, we replace $\hat{\mathbb{H}}$ with its conditional expectation given (\mathbf{y}, \mathbf{Z}) , i.e., $\mathbb{H} = \sigma_x^2 (\mathbf{1}, \mathbf{Z}_{\text{top}(k)})^\top (\mathbf{1}, \mathbf{Z}_{\text{top}(k)})$ with σ_x^2 being the conditional variance of X given Z . Then the test statistics of the resampling-free version of d₁CRT can be constructed as $\|\mathbb{H}^{-1} \tilde{\mathbf{Z}}_{\text{top}(k)} \boldsymbol{\epsilon}_x\|_2^2$. Conditional on (\mathbf{y}, \mathbf{Z}) , it is a quadratic form of the gaussian vector $\boldsymbol{\epsilon}_x$ under the null. Accurate and efficient computational methods have been proposed to handle such problems (see, e.g., Imhof (1961); Davies (1980); Liu et al. (2009)). We use the method proposed by Imhof (1961) and realized by R package `CompQuadForm` (Duchesne and De Micheaux, 2010) to compute the p -value of $\|\mathbb{H}^{-1} \tilde{\mathbf{Z}}_{\text{top}(k)} \boldsymbol{\epsilon}_x\|_2^2$.

B.2 Resampling-free dCRT with non-Gaussian X

Let $\Phi(\cdot)$ denote the cumulative distribution function (CDF) of the standard normal distribution and denote by $\sigma_i^2 = \text{Var}(X_i | Z_i)$. In Algorithm A1, we describe how to transform non-Gaussian X to be Gaussian with the same conditional variance, so that the resampling-free dCRT (for certain statistics) can be applied. Lemma A1 establishes the properties that make \mathbf{u} a good Gaussian stand-in for $\mathbf{x} - \mathbf{d}_x$, so that it can be used in a test statistic T in the same way as $\mathbf{x} - \mathbf{d}_x$ while being amenable to the resampling-free speedup.

Lemma A1. *The U_i output by Algorithm A1 are (i) monotonically increasing in X_i , (ii) distributed as $\mathcal{N}(0, \sigma_i^2)$ given Z_i , and (iii) independent from Z_i .*

Algorithm A1 Gaussian transformation.

if X is continuous with conditional CDF $F(x|Z)$, **then**

For $i = 1, 2, \dots, n$: let $U_i = \sigma_i \Phi^{-1}(F(X_i | Z_i))$.

end if

if X is discrete and supported on $\mathcal{X} = \{a_k : k \in K\}$ where $K \subseteq \mathbb{N}$ is some set of indices, $a_{k_1} < a_{k_2}$ for all $k_1 < k_2$ and $\mathbb{P}(X_i = a_k | Z_i) \neq 0$ for all $k \in K$, **then**

For $i = 1, 2, \dots, n$: if $X_i = a_k$, draw V_i uniformly from $[\mathbb{P}(X_i < a_k | Z_i), \mathbb{P}(X_i \leq a_k | Z_i)]$ and let $U_i = \sigma_i \Phi^{-1}(V_i)$.

end if

Output $\mathbf{u} = (U_1, U_2, \dots, U_n)^\top$.

Proof. For (i), when X_i is continuous, we note that both $\Phi(x)$ and $F(x|Z_i)$ are increasing and this implies U_i is unique and monotonically increasing with X_i . When X_i is discrete, noting that the range of V_i does not intersect as X_i takes different values and the range of V_i is increasing with X_i , we again have that U_i is monotonically increasing with X_i .

For (ii), when X_i is continuous, let $V_i = F(X_i | Z_i)$ and when X_i is discrete, let V_i be defined as in Algorithm A1. Since V_i is uniformly distributed on $[0, 1]$ conditional on Z_i , we have that for any $u \in \mathbb{R}$,

$$\begin{aligned} \mathbb{P}(U_i \leq u | Z_i) &= \mathbb{P}(\Phi(U_i/\sigma_i) \leq \Phi(u/\sigma_i) | Z_i) \\ &= \mathbb{P}(V_i \leq \Phi(u/\sigma_i) | Z_i) = \Phi(u/\sigma_i), \end{aligned}$$

which indicates that $\mathbb{P}(U_i/\sigma_i \leq v | Z_i) = \Phi(v)$ and $U_i \sim \mathcal{N}(0, \sigma_i^2)$. Also, we have $\mathbb{P}(U_i/\sigma_i \leq v) = \Phi(v) = \mathbb{P}(U_i/\sigma_i \leq v | Z_i)$ for all $v \in \mathbb{R}$, which indicates that $U_i/\sigma_i \perp\!\!\!\perp Z_i$. \square

C Simulation results

In this section, we present the details of the simulations summarized in Section 4. Source code for conducting dCRT and other benchmark methods in our simulation studies can be found at <https://github.com/moleibobliu/Distillation-CRT>.

C.1 Method implementation details

We describe here the implementation choices and tuning parameters used for the main methods employed in our simulations; these descriptions apply everywhere to the simulated methods unless specifically stated otherwise. For many of our methods we use the LASSO, which is implemented in the R package `glmnet` with `family="binomial"` if Y is binary and `family="gaussian"` otherwise, and penalty parameter selected by 10-fold cross-validation.

The d_0 CRT and d_1 CRT are the resampling-free versions of Examples 1 and 2, respectively. The dimension k in Examples 2 is set as $k = 2 \log(p)$. When we combine the dCRT methods with CDR from Section 3.2, the screening is done by running the 10-fold-cross-validated LASSO and keeping only the covariates with nonzero fitted coefficients.

The other methods we include are HRT, DML, GCM, and knockoff (the last only in multiple testing simulations). We implement the HRT of Algorithm 1 in Tansey et al. (2018) with linear model fitted by the LASSO, empirical risk function set to logistic loss for binary Y and sum of squared error otherwise, and a data split of 50%-50%. When implementing DML and GCM, we use our assumed exact model- X knowledge to construct the exact partial residual for each covariate, and

use the LASSO on (\mathbf{y}, \mathbf{Z}) to obtain the partial residuals for Y . For DML, we use 8-fold cross-fitting. In multiple testing simulations, BH is applied to the p -values of all methods except knockoffs. As we set $p \leq 800$ and FDR level $\alpha = 0.1$ for multiple testing, we set of the number of resamples $M = 50,000$ for the CRT approaches (CRT, HRT, non-resampling-free dCRTs). This choice was made to ensure these methods’ powers are not affected by M , since $M/5 = 10,000 > p/\alpha$, the smallest possible BH cutoff in our simulations. The only exception is in Appendix C.3 where p reached as high as 3,200, and there we choose $M = 200,000$ to ensure $M/5 > p/\alpha$. For single hypothesis testing simulations where the significance level was 0.05, we set $M = 2,000$ to ensure that we still have $M > 1/0.05$. For knockoffs, we use the LASSO coefficient difference statistics as defined in the (3.6) of Candès et al. (2018) and the “knockoffs+” threshold.

C.2 Moderate size data simulation

We first compare the dCRT with the original CRT procedure in Candès et al. (2018). We generate Gaussian covariates as AR(0.5), i.e., auto-regressive of order 1, with autocorrelation coefficient 0.5. The true model for Y is chosen as either a Gaussian linear model with unit residual variance or a logistic regression model, and in either case the coefficient vector was set to have s nonzero entries of equal magnitude ν and random signs (each independently having equal probability of being positive or negative). We pursue a multiple testing goal of selecting non-null variables while controlling the FDR at level $\alpha = 0.1$.

In addition to the methods described in Appendix C.1, we implement the original CRT with three different test statistics: the fitted coefficients of a linear or logistic LASSO regression, elastic net (Zou and Hastie, 2005) regression (penalty $\lambda(\|\boldsymbol{\beta}\|_1 + \|\boldsymbol{\beta}\|_2^2/2)$), and adaptive LASSO regression (Zou, 2006; Huang et al., 2008), each tuned with 10-fold cross-validation. Due to the high computational burden of these CRTs, we focus on moderate size data with $n = 300$, $p = 300$ and the sparsity level $s = 30$ and vary ν to observe a range of powers.

The resulting average power in the linear and logistic settings is plotted against the signal magnitude ν in Figure A1, and the FDR plots are presented in Appendix C.11. The operating characteristics of DML and GCM in this simulation are nearly indistinguishable from that of d_0 CRT because their constructions are very similar in this simulation, so we omit them from Figure A1. All methods control the FDR. The d_0 CRT and d_1 CRT significantly outperform knockoffs and the HRT and they have comparable or even slightly higher power than the all the CRT methods. The d_1 CRT has slightly less power than the d_0 CRT due to its allowance of interaction effects, since the true model is exactly additive.

To study and compare the computational efficiency of the methods, we present in Table A1 the average computation time of the methods, with all algorithms implemented in R. Compared with the original CRT procedures, the dCRTs drastically reduce the computation time and are thus much more user-friendly. Knockoffs and the HRT use less time than dCRT because they only fit a high dimensional regression for one time.

Average computation times (minutes)

	d_0 CRT	d_1 CRT	knockoff	HRT	CRT(LASSO)	CRT(ElaNet)	CRT(Ada)
Linear	0.5	0.5	0.1	0.2	259.3	301.4	268.1
Logistic	1.1	1.2	0.04	0.4	205.4	333.0	279.6

Table A1: Average computation times (in minutes) of the $n = p = 300$ simulations of Appendix C.2.

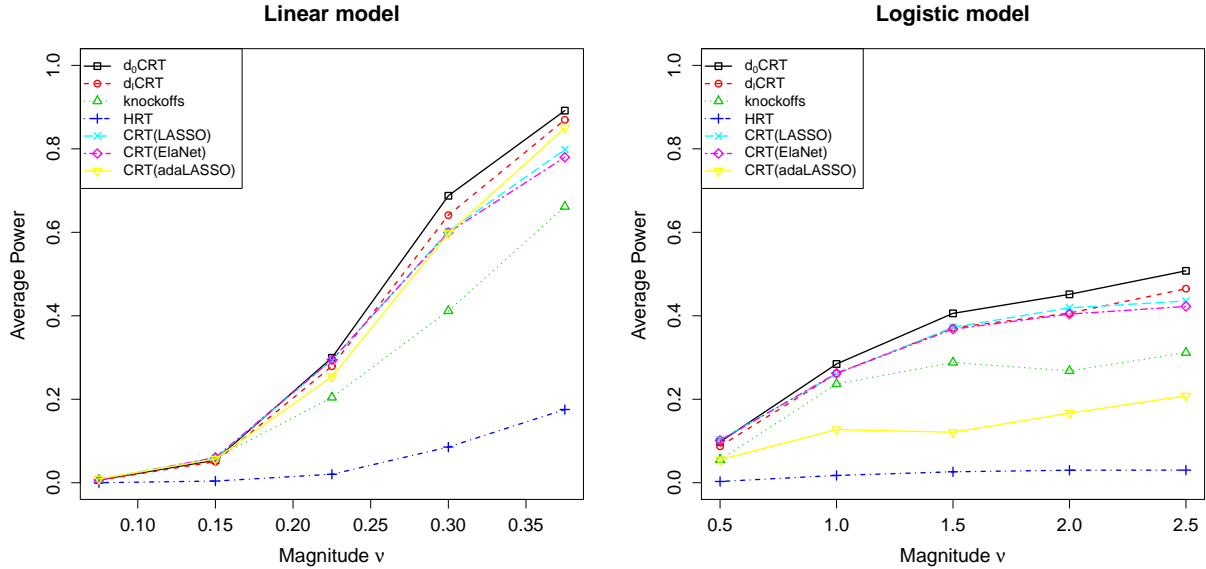


Figure A1: Average powers of the $n = p = 300$ simulation of Appendix C.2. All standard errors are below 0.01.

C.3 Large size data simulation

In this section, we conduct simulation studies of a scale beyond the CRT’s computational feasibility, and hence focus on the remaining methods whose computation stays manageable. As a baseline, we set $n = p = 800$, again use AR(1) covariates with autocorrelation 0.5, generate Y from Gaussian linear model with unit residual variance, and use a coefficient vector with $s = 50$ nonzero entries of equal magnitude $\nu = 0.175$ (chosen to make the power around 0.5) and random signs (each independently having equal probability of being positive or negative). We again pursue a multiple testing goal with nominal FDR $\alpha = 0.1$.

Each of the four average power plots in Figure A2, varies one the parameters (ν , n , p , or s) from this baseline simulation setup, with the ranges given by the x-axes. The two dCRTs have similar performance and both of them outperform knockoffs and the HRT. When the sparsity level s is below 10, power of the knockoff drops to 0 because of the effect from Appendix A. Both DML and GCM have very similar power to the d_0 CRT and are again omitted.

We present the average computation times when $n = 800$, $p = 800$ and $s = 50$ in Table A2. Knockoffs and HRT still run faster than the dCRT methods since they only fit high dimensional model once in the whole procedure.

Average computation times (minutes)			
d_0 CRT	d_1 CRT	knockoff	HRT
9.3	9.7	0.8	4.8

Table A2: Average computation times (in minutes) of the $n = p = 300$ simulations of Appendix C.3.

We now study varying the covariate and response models from this same baseline simulation. First we generate Gaussian covariates with covariance structure set as AR(1) with autocorrelations 0.25, 0.5, and 0.75, and equicorrelated with correlations 0.15, 0.3, and 0.45. Second we generate Y from three additional models given by:

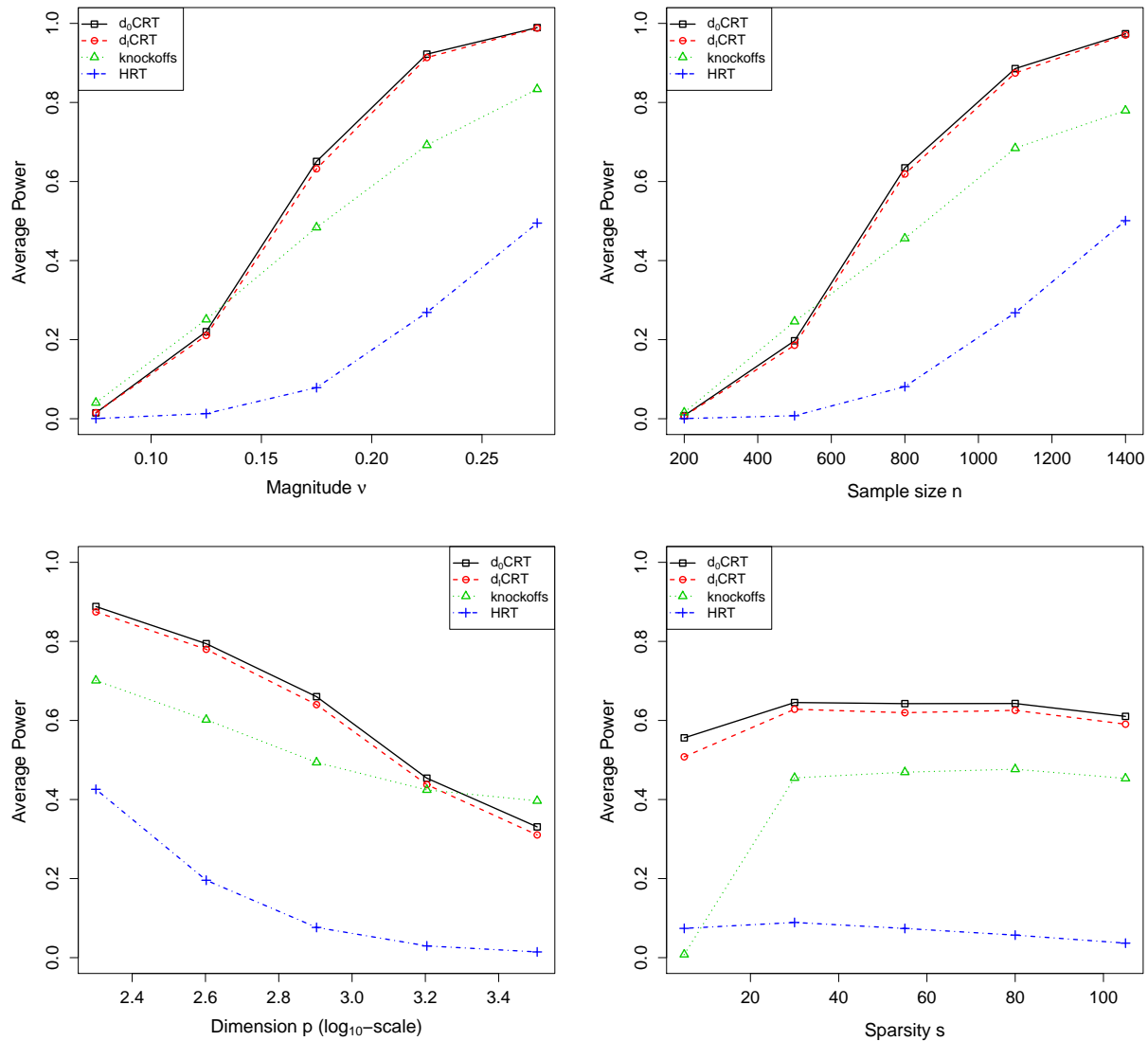


Figure A2: Average powers of the large scale simulations of Appendix C.3 that vary the coefficient magnitude, sample size, dimension, and coefficient sparsity. All standard errors are below 0.01.

- (i) **Poisson model:** Y is generated from a Poisson GLM with the same coefficient vector as the baseline model.
- (ii) **Logistic model:** Y is generated from a logistic regression with the same coefficient vector as the baseline model except $\nu = 0.5$.
- (iii) **Polynomial model:** Y is generated from a Gaussian model with conditional mean given by a polynomial that starts from the baseline model with $\nu = 0.105$ and takes each covariate with a nonzero coefficient and adds a term equal to 0.3 times its cube.

The signal magnitudes of each setting are chosen to make the powers of the main methods close to 0.5, for convenience of comparison. Note that under (i) and (iii), we still fit linear LASSO, though the model is wrong. The resulting average powers of both these simulations are plotted in Figure A3. The d_0 CRT and d_1 CRT have significantly larger power than HRT and knockoff in almost all settings, with the exception being the highly-autocorrelated design. Again, all the methods control FDR properly with the desired level 0.1 in the numerical studies corresponding to Figures A2 and A3, and we present the FDR plot in Appendix C.11.

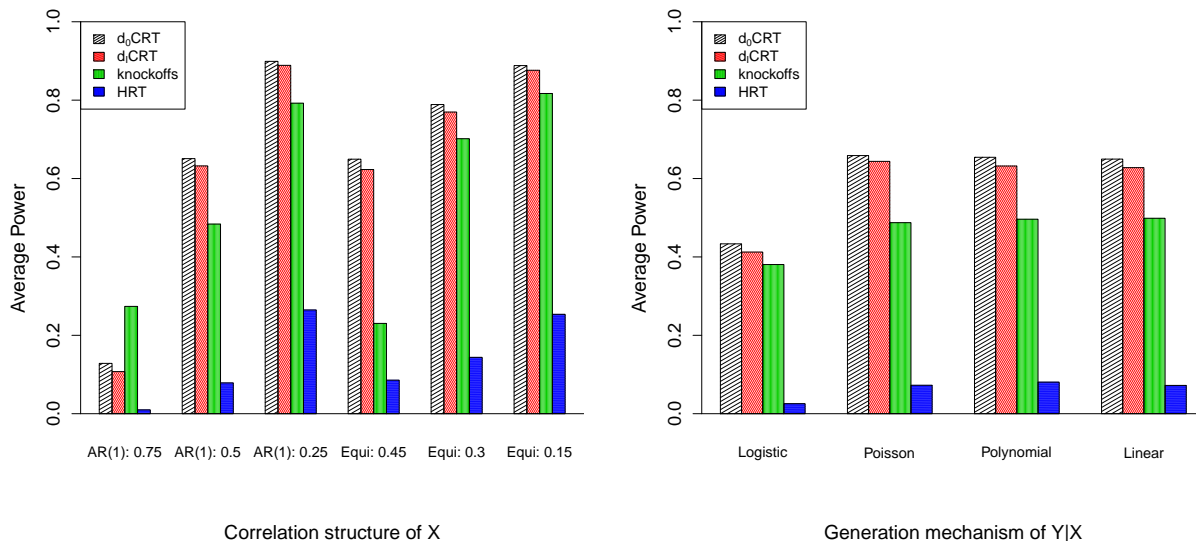


Figure A3: Average powers of the large scale simulations of Appendix C.3 that vary the covariate and response models. All standard errors are below 0.01.

C.4 Comparing d CRT with DML and GCM

As already mentioned, the construction of the resampling-free d_0 CRT ends up being quite similar to the DML proposed by Chernozhukov et al. (2016) or the GCM in Shah and Peters (2018) when X is Gaussian, and hence d_0 CRT and DML/GCM produced similar results in previous settings. However, we remind the reader that both DML and GCM rely on asymptotic normality and hence require both large samples and well-behaved tails for validity, unlike the CRT-based methods including the d CRT and HRT which are exact for any data distribution.

We demonstrate this difference by setting $n = 30$, $p = 100$ and drawing each covariate independently from a Laplace distribution with mean 0 and variance $2/9$. We generate Y from a linear

model with the residual ϵ also drawn from the Laplace distribution of mean 0 and variance 1/2. Our target is again multiple testing with FDR level 0.1. We implement HRT, DML, GCM and dCRT. Again for fair comparison, we plug in the true conditional mean and variance of X when running DML and GCM. The resulting FDRs are presented in Figure A4. Both DML and GCM have FDR level substantially above the nominal 0.1 under all magnitudes, while HRT and dCRT still control the FDR well below 0.1 (as guaranteed by Theorem 1).

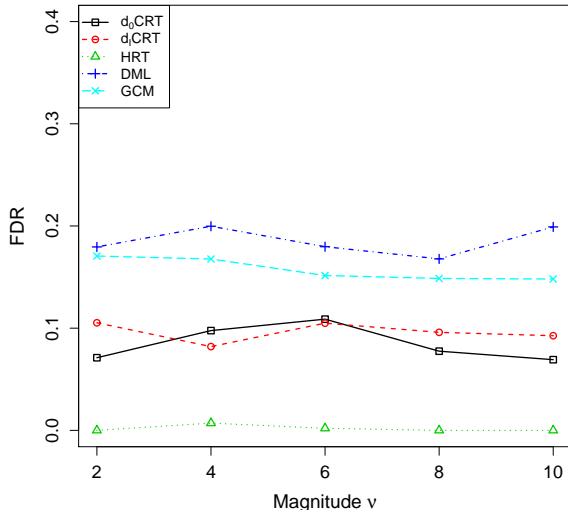


Figure A4: False discovery rates of the simulation in Appendix C.4 comparing computationally efficient CRT methods to DML and GCM. All standard errors are below 0.01.

C.5 Power improvement of the d₁CRT in the presence of interactions

All previous simulations have shown similar, if slightly worse, performance for the d₁CRT compared to the d₀CRT. This is because the models have all been additive (technically a logistic regression model is not additive, but the logistic-regression-derived statistics used by both dCRT methods fit to the logistic-transformed Y , which does follow an additive model). To demonstrate the benefits of the d₁CRT to characterize more complex effects, we conduct here a non-additive simulation with first-order interactions that obey the hierarchy principle described in Section 2.3.2. We take $n = p = 800$ and generate $(X, Z^T)^T$ from AR(1) with autocorrelation 0.5. Letting $\mu(X, Z) = \nu(X + \sum_{k=1}^5 Z_{j_k} + 1.5X \sum_{k=1}^5 Z_{j_k})$ with j_1, \dots, j_5 randomly picked from $\{1, 2, \dots, 799\}$, we generate Y either from a Gaussian model with conditional mean given by $\mu(X, Z)$ or from a Bernoulli model with $\log(\mathbb{P}(Y = 1 | X, Z) / \mathbb{P}(Y = 0 | X, Z)) = \mu(X, Z)$. The target is to test the single hypothesis $Y \perp\!\!\!\perp X | Z$ at level 0.05 (hence knockoffs does not apply). Figure A5 shows the powers of the d₀CRT, d₁CRT, and HRT (again, DML/GCM are not shown as they closely match the d₀CRT curves). As is expected, d₁CRT has substantially higher power than d₀CRT and DML/GCM.

C.6 Stability of the d₁CRT to the choice of k

In this section, we study the sensitivity of d₁CRT to the choice of k defined in Example 2. We simulate the d₁CRT in the baseline setting (linear model) of Section C.3 and the linear interaction

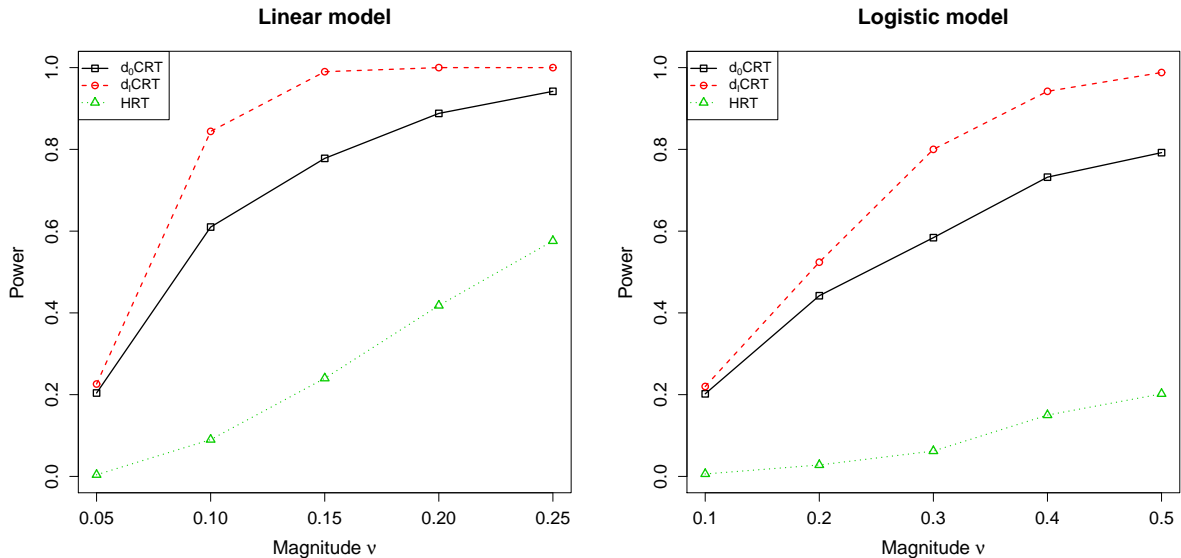


Figure A5: Powers of the simulations in Appendix C.5 comparing methods in the presence of interactions. All standard errors are below 0.03.

model setting of Section C.5 for varying choices of k (in both settings, the default $k = 2 \log(p) \approx 13$). The results in Figure A6 show that the choice of k has nearly no impact on the power of the d_1 CRT in the linear model setting. In the interaction setting, the power of the d_1 CRT decreases with k for $k > 5$ since there are only 5 true interactions in the model, but the trend is quite gradual and the d_1 CRT’s power stays above that of d_0 CRT through $k = 22$.

C.7 A random-forest-based d_1 CRT

Examples 1 and 2 are inherently rooted in generalized linear models (GLMs), and we expect them to perform well in situations where a GLM captures much of the interesting dependence between Y and X . But there is nothing limiting the d CRT’s application to such settings, and in this section we demonstrate the power of a random-forest-based d_1 CRT in a setting that is far from a GLM.

Example 3 (Random-forest-based d_1 CRT). Let $\mathbf{d}_{y,1}$ be the fitted predictions from a random forest fitting \mathbf{y} to \mathbf{Z} , let $\mathbf{d}_{y,-1}$ be the columns of \mathbf{Z} corresponding to the k largest values of the default variable importance measure in the R package *randomForest*, and let $T(\mathbf{y}, \mathbf{x}, \mathbf{d}_y, \mathbf{d}_x)$ fit a random forest of \mathbf{y} on $\mathbf{x} - \mathbf{d}_x$ and \mathbf{d}_y and return the default variable importance measure for $\mathbf{x} - \mathbf{d}_x$.

We take $n = p = 800$ and $(X, Z^T)^T$ as following an AR(1) model with autocorrelation 0.5. We choose a conditional model for Y in which the magnitude of the effect of X on Y is heterogeneous and varies with Z : $\mu(X, Z) = \nu[0.5X^2 + \sin(0.5\pi X)](0.3 + \sum_{k=1}^5 Z_{j_k})$, and Y is standard normal noise added to $\mu(X, Z)$. We simulate tests of $Y \perp\!\!\!\perp X \mid Z$ at significance 0.05 and plot the results in Figure A7. The random-forest-based d_1 CRT is denoted by “ d_1 CRT (RF)” and uses 100 trees for distillation and 30 trees for computation of T . The additional function-approximation flexibility of random forests imparts a substantial gain in power compared to d_0 CRT, d_1 CRT, HRT, DML, and GCM (latter two not shown due to overlap with d_0 CRT) which are all implemented based on GLMs.

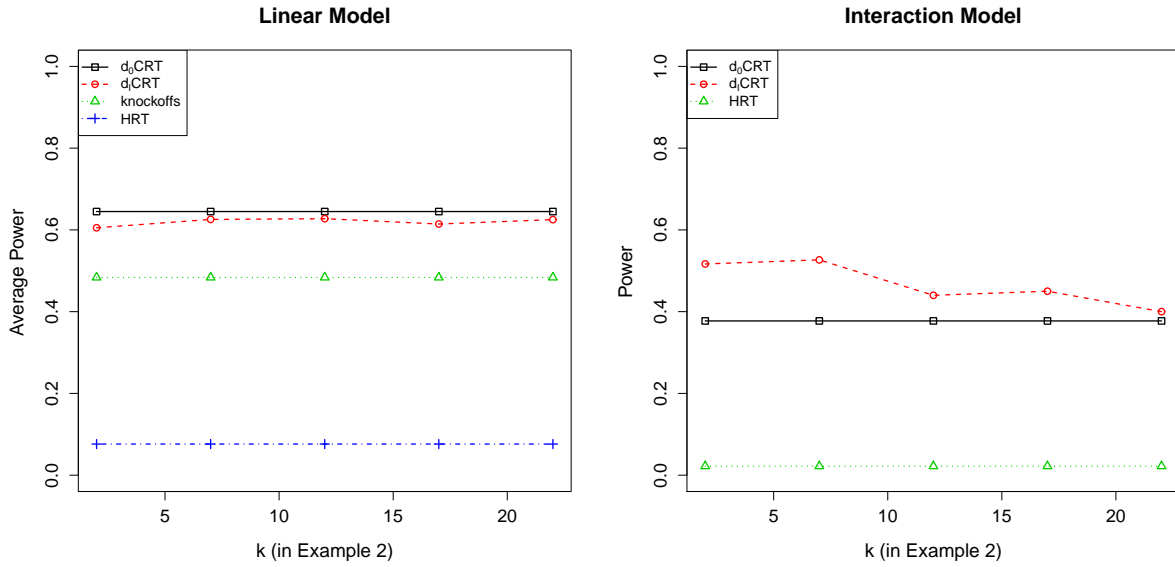


Figure A6: Powers of the simulation in Appendix C.6 evaluating the stability of the d_1 CRT to the choice of k . All standard errors are below 0.03.

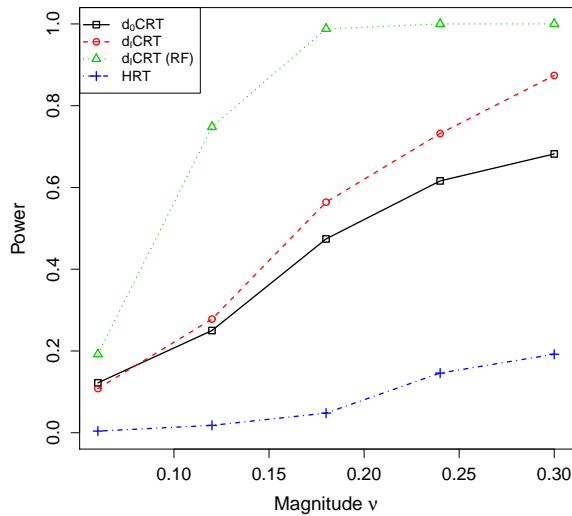


Figure A7: Powers of the simulations in Appendix C.7 demonstrating a random-forest-based d_1 CRT. All standard errors are below 0.03.

C.8 Robustness

We designed numerical experiments to study the robustness of the dCRTs, i.e., whether the methods still control Type 1 error and have power when the $X | Z$ distribution is misspecified.

C.8.1 Known first and second moments

We first consider the case when one has no knowledge of the conditional distribution of $X | Z$ except its first two moments, and simply treats $X | Z$ as conditionally Gaussian with matching moments. We let $n = p = 800$ and generate $Z = (Z_1, Z_2, \dots, Z_{799})^\top$ from a Gaussian AR(1) model with autocorrelation 0.5 and sample X as conditionally Poisson:

$$X = 0.15 \sum_{j=1}^{50} \varphi_j Z_j + \delta, \quad \text{where } \delta = \frac{O - r}{\sqrt{r}} \quad \text{with } O | Z \sim \text{Poi}(r),$$

where each φ_j is independently and uniformly drawn from $\{-1, 1\}$ and $\text{Poi}(r)$ represents the Poisson distribution with mean r . When r is small, $(O - r)/\sqrt{r}$ is quite skewed with its tail behaviour highly different from Gaussian while as r becomes larger, $(O - r)/\sqrt{r}$ converges to a $\mathcal{N}(0, 1)$. We run the dCRT as if $\delta \sim \mathcal{N}(0, 1)$, and hence r measures the degree of misspecification (lower r corresponds to more misspecification). For Y , we use linear or logistic model linked with $\nu X + 0.15 \sum_{j=1}^{50} \psi_j Z_j$.

Our target is to test for $Y \perp\!\!\!\perp X | Z$ with level 0.05. To study the performance in Type 1 error control we set $\nu = 0$, while to study the power we let $\nu = 0.1$ for linear model and $\nu = 0.2$ for logistic model. Methods in comparison include d_0 CRT, d_1 CRT, HRT, DML, and GCM with the same specification as the previous section except that $X - \mathbb{E}[X|Z]$ is approximated as $\mathcal{N}(0, 1)$ when modelling X . The resulting Type 1 error and power versus $\log_2(r)$ are plotted in Figure A8. Even when r is as small as 0.5, the Type 1 error of the dCRTs (and in fact all the methods; again DML and GCM not plotted because they match d_0 CRT) remain below their nominal level and their powers are relatively similar to the nearly-well-specified setting of $r = 64$.

C.8.2 In-sample-estimated moments

Next, we study the case when one knows a model family for $X | Z$ but needs to estimate its parameters in-sample. Again, we set $n = 800$, $p = 800$, $s = 50$, generate the covariates from a Gaussian AR(1) distribution with autocorrelation 0.5 and generate Y from a linear model with magnitude $\nu = 0.175$ or logistic model with magnitude $\nu = 0.5$, which again makes the power roughly 0.5. Then, as part of our dCRT procedures, we use the $n = 800$ samples to estimate the precision matrix of the covariates. For this purpose, we implement the graphical LASSO (Friedman et al., 2008, gLASSO) tuned by cross-validation. Given the true sparsity of this particular covariate model, the gLASSO does relatively well, so we also try mixing its covariance matrix estimate $\hat{\Sigma}_g$ with the sample covariance matrix $\hat{\Sigma}$, which is a very poor estimate since $n = p$.

$$\hat{\Sigma}_m = D\{v\hat{\Sigma} + (1 - v)\hat{\Sigma}_g\}D,$$

where $v \in [0, 1)$ is a proportion parameter controlling the mixture of the two estimates and $D = \text{diag}\{d_1, d_2, \dots, d_p\}$ is a $p \times p$ diagonal matrix, where d_j is the ratio of the estimated conditional variance by inverting $v\hat{\Sigma} + (1 - v)\hat{\Sigma}_g$ and that estimated using the mean squared residuals. Here D is just used to ensure that the estimated conditional variance is close to its sample mean squared residual. By changing v , we are able to inspect the performance of the dCRT as the quality of our covariance estimation varies.

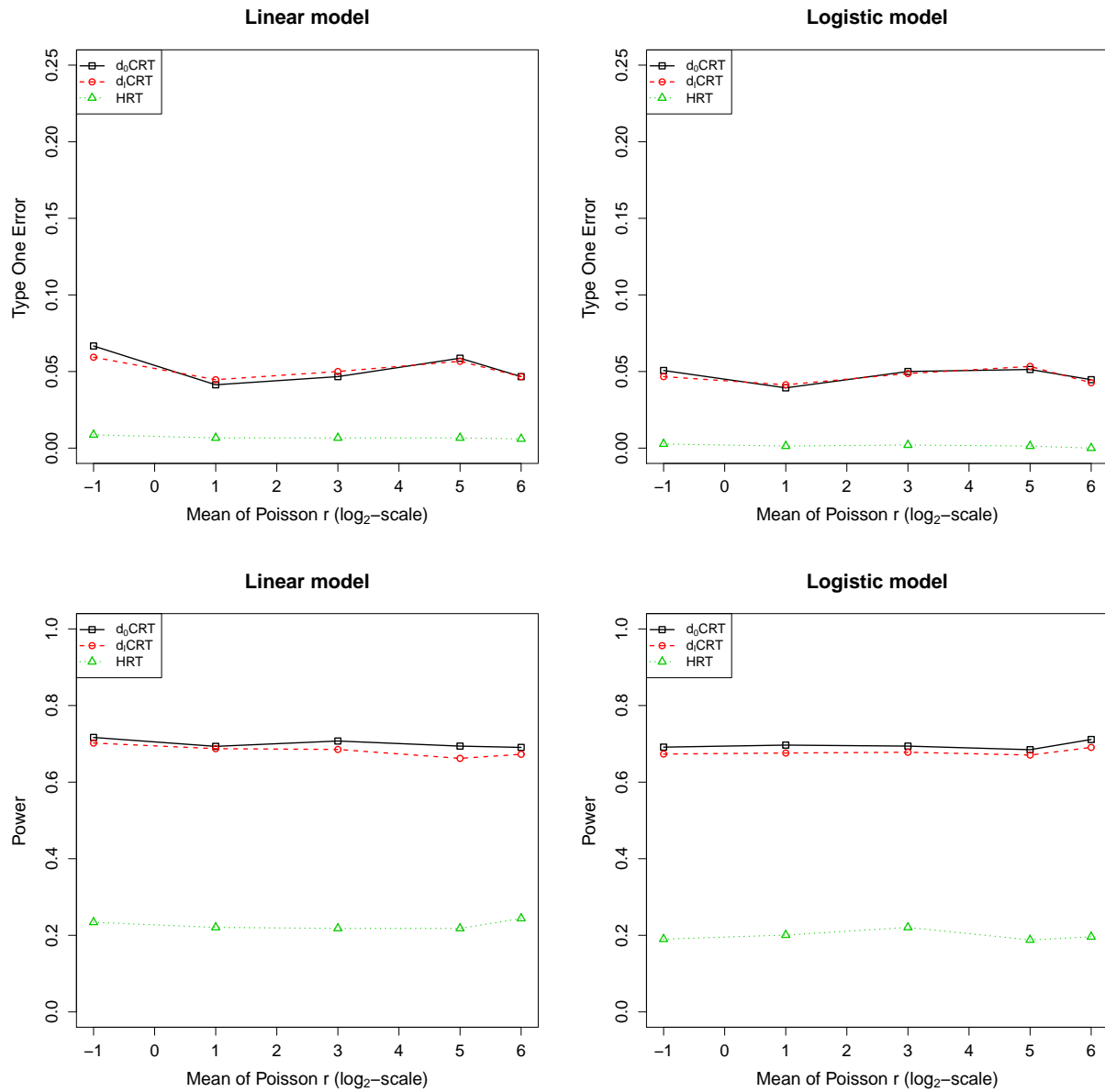


Figure A8: Type 1 error rates and powers of the simulations in Appendix C.8.1 measuring robustness to misspecification in terms of the parameter r . All standard errors are below 0.03.

The goal of the simulation is is controlled variable selection with FDR level 0.1. The resulting FDR and power versus ν are presented in Figure A9. As the estimation error gets worse, knockoffs becomes conservative and its FDR and power drop. However, the dCRTs and GCM/DML (which are not shown but match the d_0 CRT) become slightly anticonservative as the estimation gets worse, achieving a somewhat inflated FDR but maintaining closer power to the setting with better estimation at $\nu = 0$, where they appear to behave exactly as if the covariance matrix were known exactly.

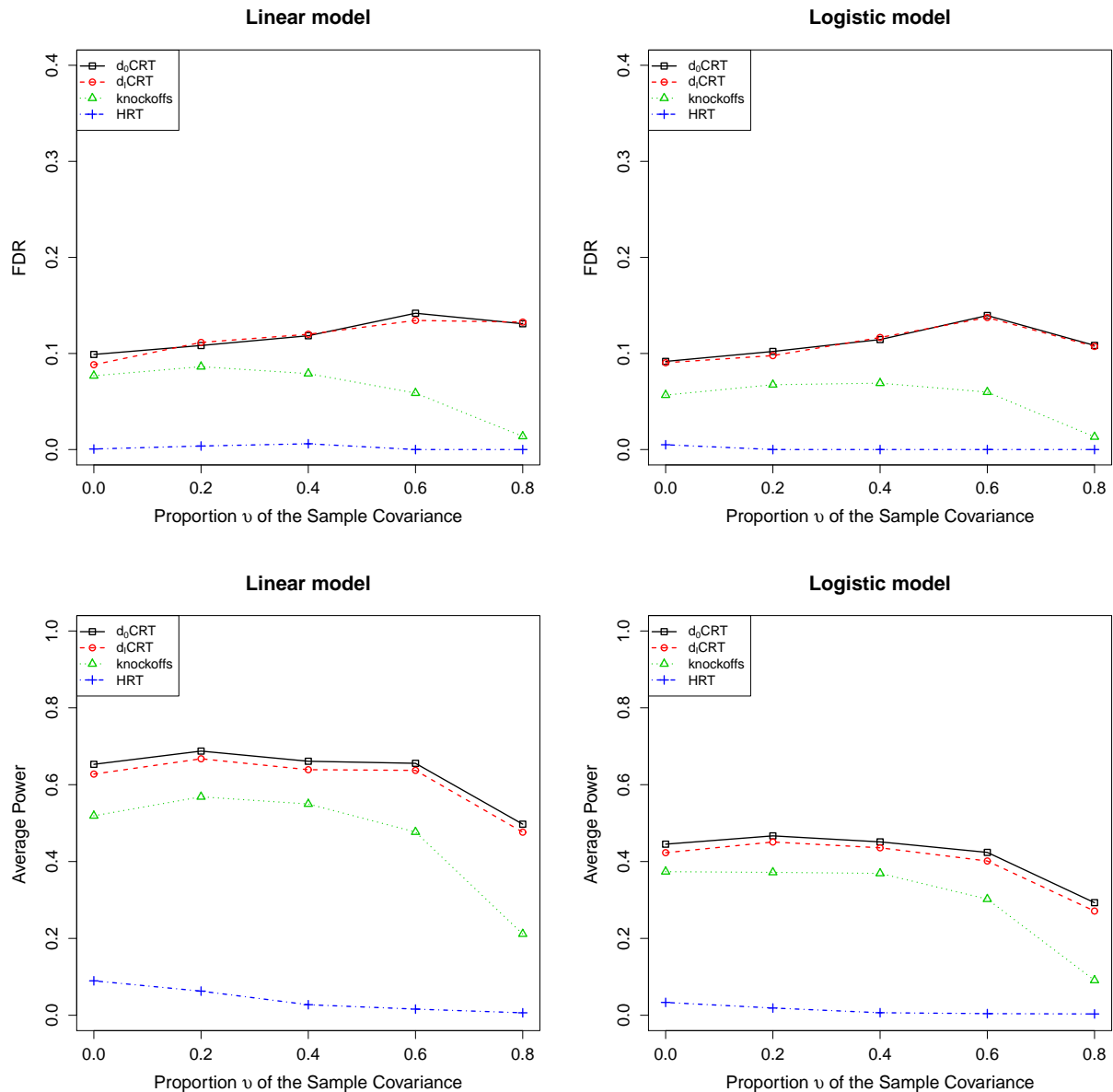


Figure A9: FDRs and average powers of the simulations in Appendix C.8.2 measuring robustness to in-sample estimation of the covariate covariance matrix. All standard errors are below 0.01.

C.9 Measuring the effect of the resampling-free modification

C.9.1 Gaussian covariates

Section 3.1 proposes a resampling-free version of d_0 CRT and d_1 CRT requiring a small modification to their test statistics; we show here this modification does not affect their powers. Under the baseline setting of Section C.3 and the setting with Gaussian covariates and interactions in Section C.5, we compare the resampling-free dCRTs with their non-resampling-free versions in terms of average power. Figure A10 shows the resampling-free modification makes essentially no difference to their powers.

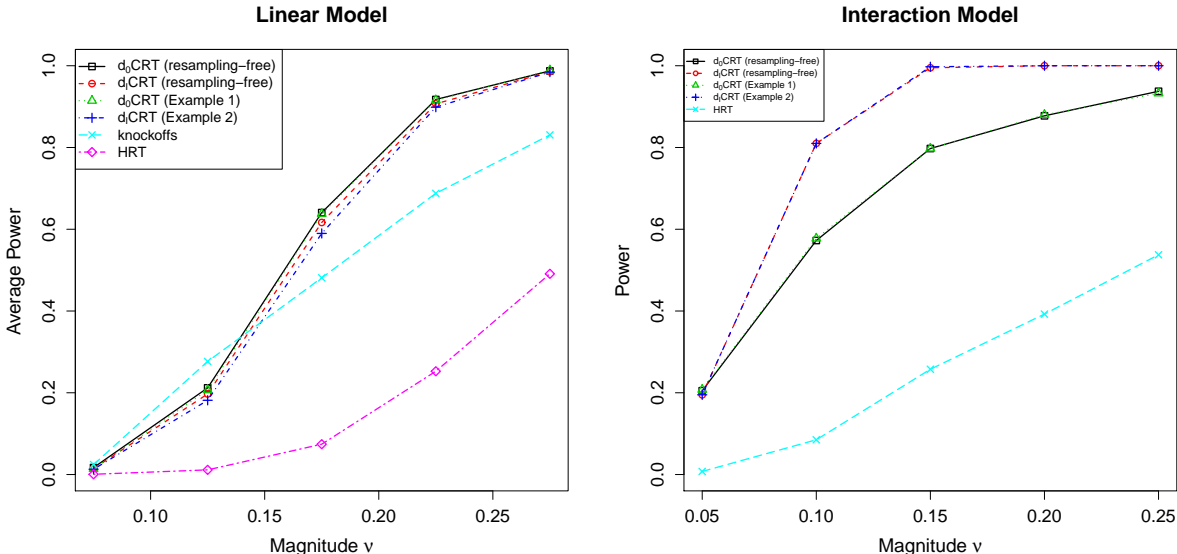


Figure A10: Powers of the simulation in Appendix C.9.1 measuring the effect of the resampling-free modification to the d_0 CRT and d_1 CRT test statistics. All standard errors are below 0.03.

We also include computation times for the baseline setting of Section C.3 in Table A3, showing that the resampling-free versions of the dCRTs confer a substantial computational savings.

Average computation times (minutes)

d_0 CRT (resampling-free)	d_0 CRT (Example 1)	d_1 CRT (resampling-free)	d_1 CRT (Example 2)	knockoff	HRT
9.3	24.7	9.7	109.6	0.8	4.8

Table A3: Average computation times (in minutes) of the linear model simulations of Appendix C.9.1.

C.9.2 Non-gaussian covariates

As we introduced in Section 3.1 and detailed in Appendix B, when $X | Z$ is non-Gaussian, it must be transformed to Gaussian in order to apply the resampling-free speedup; we examine here the effect this transformation has on power. We generate covariates i.i.d. from two different distributions: (i) Gamma with shape 3 and rate 0.5 and (ii) Bernoulli with mean 0.5. We took $n = p = 800$,

$s = 50$ and Y generated from linear (in the untransformed covariates) model and performed multiple testing for variable selection at FDR level 0.1. Our main goal is to compare the d_0 CRT of Example 1 and the d_1 CRT of Example 2 with their respective resampling-free counterparts, though we also run the HRT, knockoffs, DML, and GCM. The resulting average powers versus signal strength ν are shown in Figure A11. For Gamma X , the Gaussian transformation comes with almost no loss in power while for Bernoulli X , the resampling-free dCRTs lose substantial power but still substantially outperform the HRT. This is due to the highly non-Gaussian nature of a Bernoulli(0.5) distribution and the need for substantial exogenous randomness to be added to X to make it Gaussian. Knockoffs performs competitively with the dCRT methods in both simulations, and we attribute this to the covariate independence which allows very high-quality knockoffs to be used.

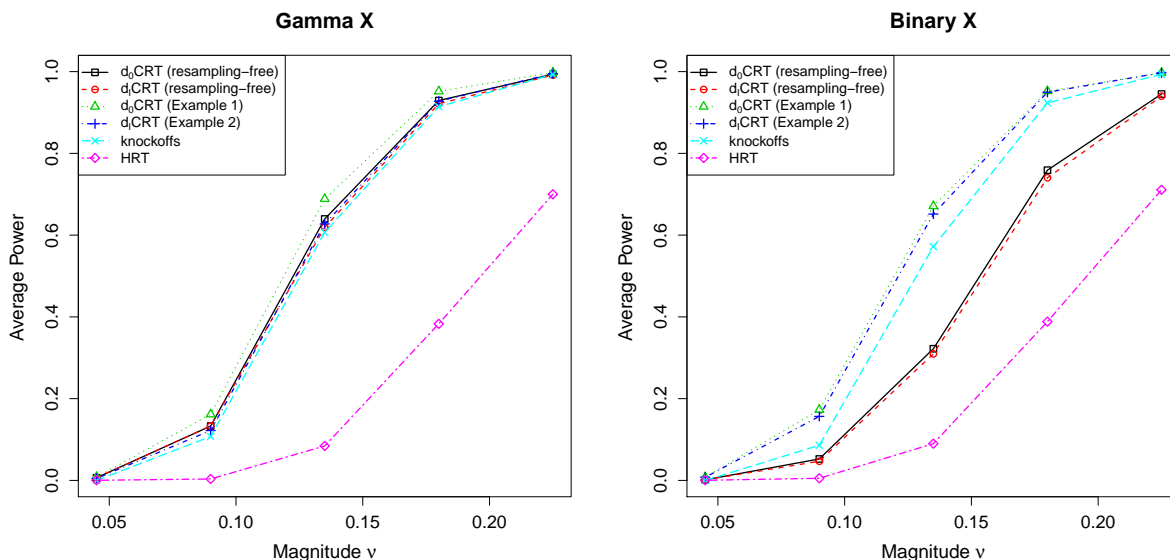


Figure A11: Powers of the simulation in Appendix C.9.2 measuring the effect of the Gaussian transformation in the resampling-free dCRTs. All standard errors are below 0.01.

C.10 Impact of CDR on computation efficiency and power

Here we demonstrate the effect of the CDR modification introduced in Section 3.2 on computation time and power. We again simulate the baseline setting in Section C.3 and compare the power and computation time of the dCRT methods with CDR with the dCRT procedures without using CDR. In Table A4 we present computation times demonstrating that CDR can substantially improve the computational efficiency of dCRT. And the corresponding average powers are shown in Figure A12, demonstrating that CDR has nearly no impact on the power of the d_0 CRT or d_1 CRT.

Average computation times (minutes)					
d_0 CRT (CDR)	d_0 CRT (full)	d_1 CRT (CDR)	d_1 CRT (full)	knockoff	HRT
9.3	43.5	9.7	44.5	0.8	4.8

Table A4: Average computation times (in minutes) of the simulations in Appendix C.10.

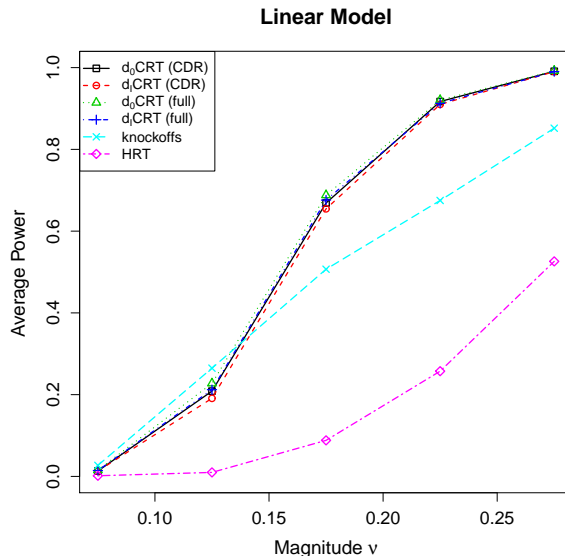


Figure A12: Average powers of the simulation in Appendix C.10 measuring the effect of the CDR modification. All standard errors are below 0.01.

C.11 Additional FDR results

We compile FDR results of our simulations with well-specified covariate distributions here. The FDR is guaranteed to be controlled by knockoffs and the p -values of the CRT procedures including the dCRTs are guaranteed to be valid, but they do not satisfy the conditions for the BH procedure to control the FDR. In practice, they do, as Figures A13–A15 show.

D Breast cancer data analysis

In this section, we present the details of our analysis of the breast cancer data set in Section 5; our code for pre-processing and analyzing the data is available at <https://github.com/moleibobliu/Distillation-C>. The list of $p = 173$ candidate genes is given in Supplementary Data 1 of Pereira et al. (2016) and can be downloaded from <https://www.nature.com/articles/ncomms11479#Sec32>. The CNA, gene expression and clinical data itself is from cBioPortal and can be downloaded from <https://www.cbioportal.org/st>. The raw cancer stage used in our response variable is from the column labeled *TUMOR_STAGE* in their table for clinical data. It consists of three categories, 1, 2 and 3 that represent the progression stage of breast cancer. Since there were relatively few observations in category 1, we merge categories 1 and 2 together, resulting in a binary response. And the samples for analysis were chosen as all the patients with ER+ given in the clinical table.

Now we introduce the procedures for modeling the covariates. To model the expression levels of each gene G_j conditional on its corresponding CNA level C_j , we follow the methods proposed and discussed in Solvang et al. (2011); Lahti et al. (2012); Leday et al. (2013) to fit a piecewise linear regression of each G_j on each C_j . Denoting the fitted residuals as \tilde{G}_j and $\tilde{\mathbf{G}} = (\tilde{G}_1, \dots, \tilde{G}_p)$ we then model $\tilde{\mathbf{G}}$ as mean-zero multivariate Gaussian and estimate its precision matrix via a similar procedure as in Section C.8.2. That is, we remove the mean of each \tilde{G}_j , fit gLASSO tuned with cross-validation to estimate the precision matrix, and finally take the inverted precision matrix estimate and multiply it by a diagonal matrix to match the conditional variance of each \tilde{G}_j with

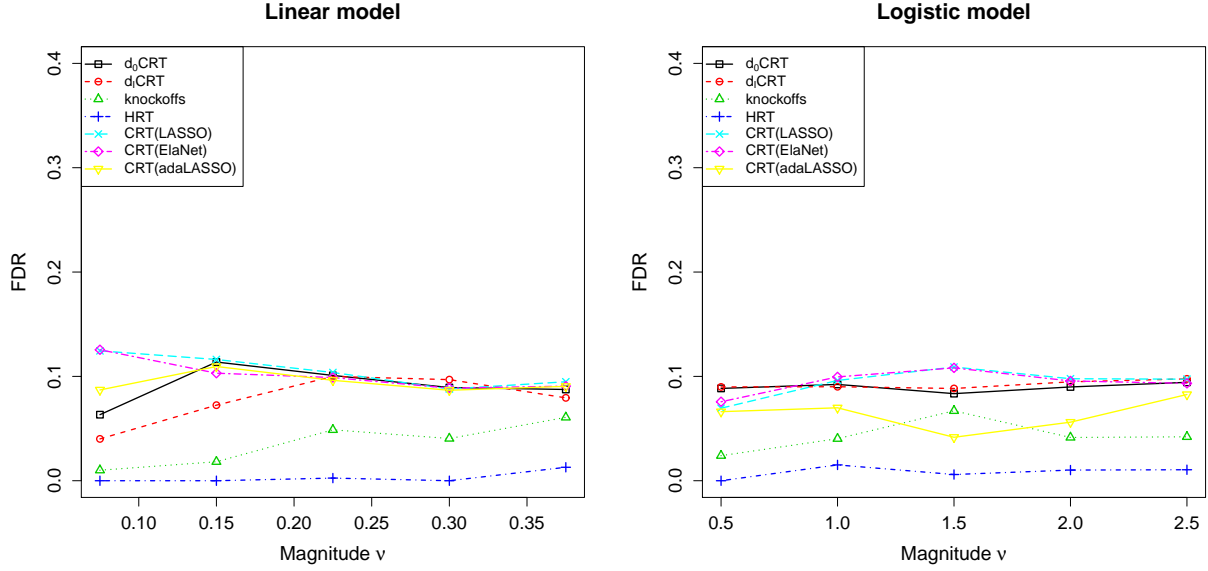


Figure A13: FDRs of the $n = p = 300$ simulation of Appendix C.2. All standard errors are below 0.01.

the mean square of its residuals.

As in the simulations, the d_0 CRT and d_1 CRT we use are the resampling-free logistic regression versions of Examples 1 and 2 along with CDR with the logistic LASSO. We also implement knockoffs, the HRT, and the original CRT as in the simulations section with analogous logistic LASSO statistics. The number of resamples for the HRT and the original CRT is set as $M = 25,000$, again satisfying $M/5 > p/\alpha$ as the FDR level α is set as 0.1.

We summarize the discovered genes and their p -values estimated by each method in Table A5.

Gene	d_0 CRT	d_1 CRT	CRT(LASSO)	HRT
<i>FBXW7</i>	9.5×10^{-4}	3.7×10^{-4}	1.8×10^{-3}	6.2×10^{-2}
<i>GPS2</i>	2.7×10^{-4}	2.3×10^{-4}	1.2×10^{-4}	8.2×10^{-3}
<i>HRAS</i>	1.8×10^{-3}	1.9×10^{-3}	2.1×10^{-3}	5.4×10^{-3}
<i>MAP3K1</i>	4.9×10^{-5}	3.0×10^{-5}	6.1×10^{-3}	1
<i>RUNX1</i>	2.5×10^{-4}	2.5×10^{-4}	2.0×10^{-4}	4.4×10^{-4}

Table A5: Selected genes and their corresponding estimated p -values; those in bold are rejected by BH at FDR level 0.1. Knockoffs selected no genes.

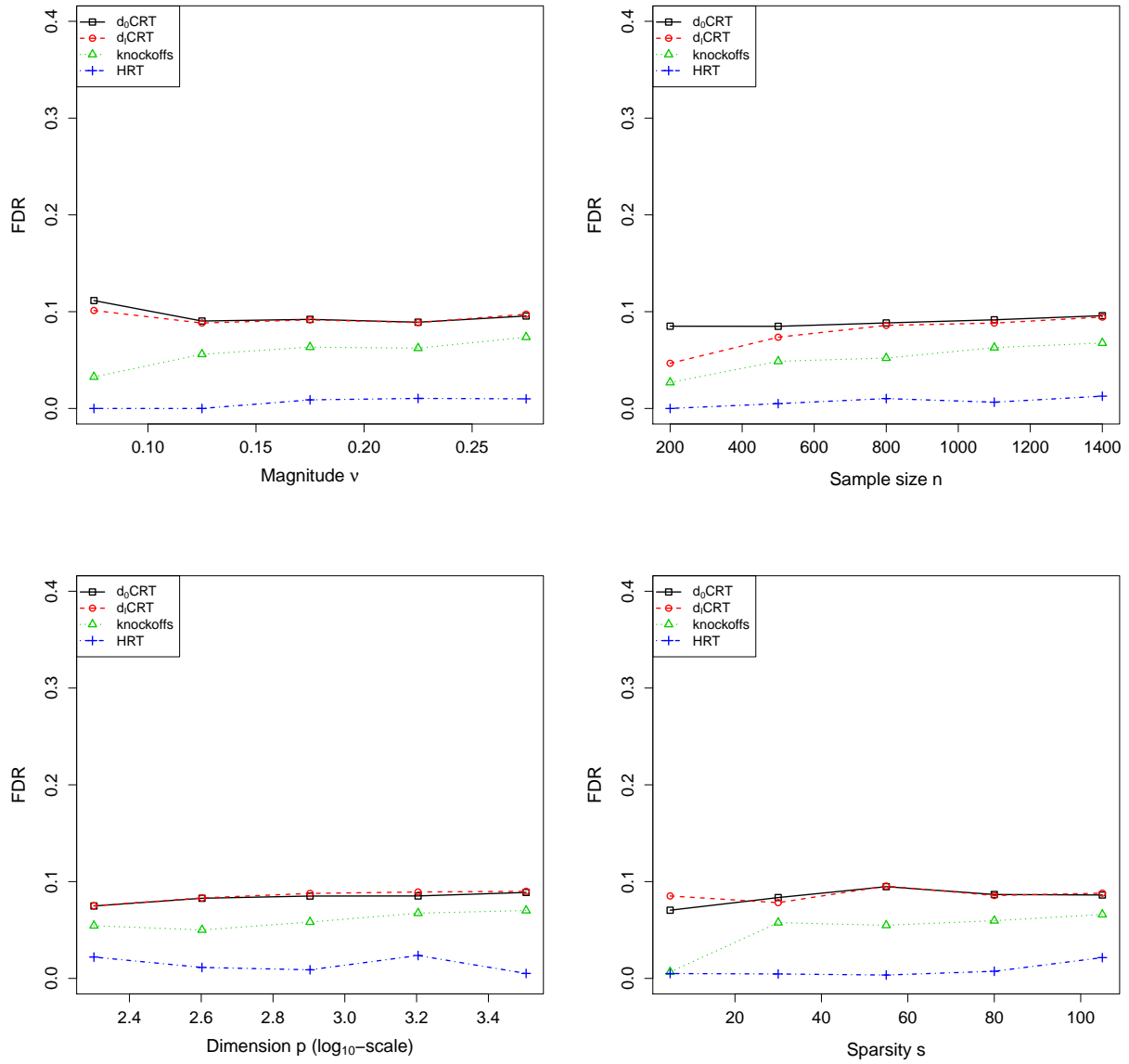


Figure A14: FDRs of the large scale simulations of Appendix C.3 that vary the coefficient magnitude, sample size, dimension, and coefficient sparsity. All standard errors are below 0.01.

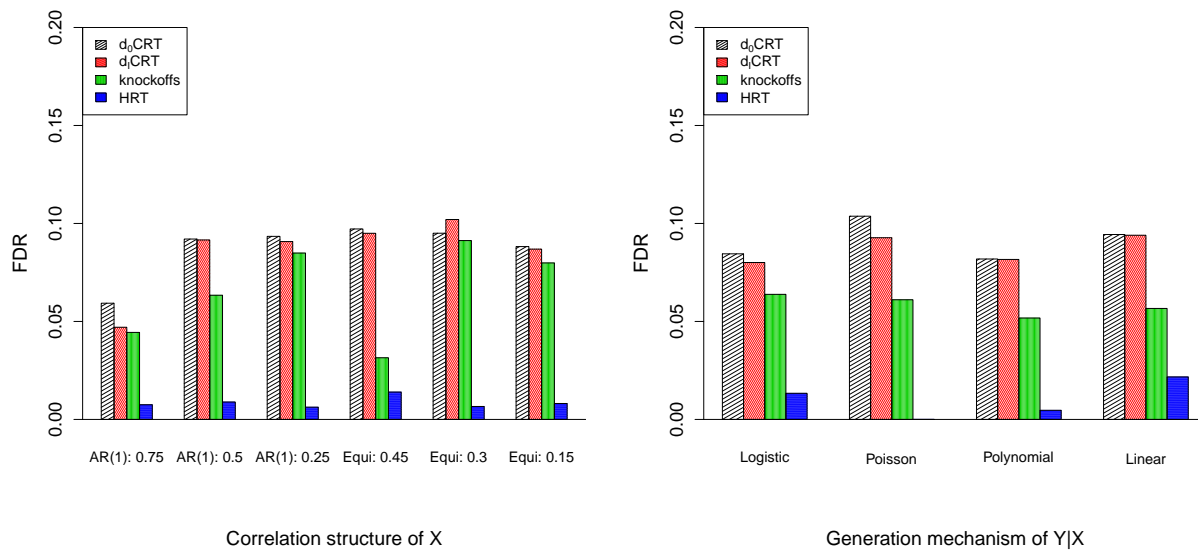


Figure A15: FDRs of the large scale simulations of Appendix C.3 that vary the covariate and response models. All standard errors are below 0.01.